THE INFLUENCE OF EFFECTIVE CONSOLIDATION STRESS ON THE NORMALIZED EXTENSION STRENGTH PROPERTIES OF RESEDIMENTED BOSTON BLUE CLAY

BY

SAFIA R. MONIZ

B.SC.(ENG) CIVIL ENGINEERING
UNIVERSITY OF THE WEST INDIES
ST. AUGUSTINE, TRINIDAD
2004

Submitted to the Department of Civil and Environmental Engineering in Partial Fulfillment of the Requirements for the Degree of Masters of Engineering in Civil and Environmental Engineering

at the

Massachusetts Institute of Technology

June 2009

Signature of Author.....
Department of Civil and Environmental Engineering
May 8, 2009

Credited by.....
John T. Germaine
Senior Lecturer of Civil and Environmental Engineering
Thesis Supervisor

Accepted by.....
Daniele Veneziano
Chairman, Departmental Committee for Graduate Students
Civil and Environmental Engineering

THE INFLUENCE OF EFFECTIVE CONSOLIDATION STRESS ON THE NORMALIZED EXTENSION STRENGTH PROPERTIES OF RESEDIMENTED BOSTON BLUE CLAY

BY

SAFIA R. MONIZ

Submitted to the Department of Civil and Environmental Engineering
On May 8, 2009 in Partial Fulfilment of the Requirements for the Degree of
Masters of Engineering in Civil and Environmental Engineering

ABSTRACT

The ability to accurately determine the undrained shear strength of cohesive soil is of particular importance to the practice of geotechnical engineering. Ladd & Foot (1974) presents a method to determine the undrained shear strength based on the concept of normalized soil parameters; called the SHANSEP (Stress History and Normalized Soil Engineering Properties) method.

Recent research at MIT has discovered a consistant variation of undrained shear parameters during triaxial compression. Undrained triaxial compression tests on RBBC (Resedimented Boston Blue Clay) have shown that the soil stiffness and strength is dependant on the vertical consolidation effective stress and that the strength behaviour does not strictly conform to a normalized framework.

The aim of this study is to explore the trend between vertical consolidation stress and the undrained shear strength behaviour in extension for cohesive soils to determine whether the normalized soil parameter concept (and hence SHANSEP) is still applicable at vertical consolidation stresses ranges of $\sigma'_v \geq$ 10 ksc (1.0MPa). To do this, a series of K_0-consolidated undrained triaxial extension tests were performed at vertical consolidation consolidation stresses ranging from 1.5 ksc (0.15 MPa) to 20 ksc (2.0MPa). Results from these tests clearly show that the undrained shear strength decreases with vertical effective stress. The undrained shear strengths decreased from 0.17 ksc to 0.15 ksc, and the friction angle decreased from 45° to 31.1° corresponding to an increase in vertical consolidation stress level. The results also show that the maximum secant modulus (E_{max}) was found to decrease exponentially with the vertical consolidation effective stress (σ'_{vc}) according to the equation: $E_{max} = 450 \times \sigma'^{0.74}_{vc}$. This relationship was proposed by Santagata (1999) and was presented as: $E_{max} \propto \sigma'^{0.74}_{vc}$.

There is not any apparent relationship between the lateral stress ratio and the vertical consolidation stress. The trends observed during shear in extension are consistent with observations made during K_0 consolidation compression testing.

Thesis Supervisor: John T. Germaine
Title: Senior Lecturer in Civil and Environmental Engineering

TABLE OF CONTENTS

LIST OF FIGURES

LIST OF TABLES

LIST OF PHOTOS

ACKNOWLEDGEMENTS

The author would like to express her gratitude to the following people who helped make this thesis a reality:

Dr. Jack Germaine, my thesis supervisor, for his guidance and dedication to my learning throughout the entire year. Dr. G answered my many questions (often asked more than once) with unwavering patience. His obvious love for his profession has been infectious as I find myself even more fascinated by laboratory testing and soil behaviour. (Dr. G was the only other person who appreciated or understood why I stayed in the lab all night to take pictures of the development of a failure plane in a soil specimen). No doubt I will be a better engineer because of him.

Naeem Abdulhadi, for teaching me the intricacies of triaxial machine MIT02, being there to answer my questions every step of they way and for helping me troubleshoot the many issues associated with triaxial testing, which always seemed to happen on a Sunday afternoon.

Geotech Associates Limited for the funding of this degree, and the directors: Martin Andrews, Andrew Bhudram, and Malcom Joab for their support of my professional development.

My friends, Therese, Ingrid, Kevin and Kate for always cheering me on. They definitely made my year at MIT, and make my life in general, a lot happier.

My friends at MIT, too many to name, in the MEng., S.M. and Phd., program: I have been honoured to have spent a year with a collection of some of the most intelligent and friendly people from all over the world. They must be thanked for sticking their heads in the lab to say hi to me every time they walked by. Those little bits of chat and those smiles made the many hours in the lab go by quickly.

Dr. Dorrell Philip, for pushing me to apply to graduate school and believing in my ability especially when I did not.

My family: My Dad and Mom, for making my education a priority in their lives, for always pushing me to keep going, being there for me no matter what, not allowing me to settle for mediocrity and for being proud of me. My sisters, Justine and Zara, for the love, support, and the very amusing teasing about my supposed nerdiness.

Safia R. Moniz

You taught me my first word,
Now I dedicate these words to you.
In loving memory of my grandmother
Jean Edith Norton Weekes
(1921 – 2007)

LIST OF SYMBOLS

Notes:
(1) Prefix Δ indicates a change.
(2) Suffix $_f$ indicates a final or failure condition.
(3) A superscript prime (') on stress indicates an effective stress.
(4) A superscript prime on a property indicates a value in terms of effective stress.

SYMBOL	DEFINITION
BASIC	Beginner's All-purpose Symbolic Instruction Code
BBC	Boston Blue Clay
CK_0UC	K_0 Consolidated Undrained Compression Test
CK_0UE	K_0 Consolidated Undrained Extension Test
CRS	Constant Rate of Strain Test
DC	Direct Current
DCDT	Direct Current Displacement Transducer
DSS	Direct Simple Shear Test
FV	Field Vane Test
K_0	Coefficient of Earth Pressure at Rest
LIR	Load Increment Ratio
LVDT	Linear Variable Differential Transformer
MIT	Massachusetts Institute of Technology
NC	Normally Consolidated
NSP	Normailized Soil Parameters
OC	Overconsolidated
OCR	Overconsolidation Ratio
PSA	Plane Strain Active Shear Test
PSP	Plane Strain Passive Test
RBBC	Resedimented Boston Blue Clay
TE	Triaxial Extension Shear Test
TX	Triaxial
U	Unconfined Compression Test
UU	Unconsolidated Undrained Compression Test
SHANSEP	Stress History and Normalized Soil Engineering Properties
VCL	Virgin Compression Line
A (A_f)	Skempton's pore pressure parameter (at failure)
B	Skempton's pore pressure parameter
c_v	Coefficient of consolidation
C_c	Compression Index
C_α	Coefficient of Secondary Compression
e	Void ratio
$E_{u(max)}$	Secant modulus (maximum)
ε	Strain
ϕ'	Peak Friction Angle
I_p	Plasticity Index
k	Hydraulic Conductivity
m	Slope of OCR vs. Shear Stress, $d\ log(S_u/\sigma_{vc}') / d\ \log OCR$

p'	Mean effective stress, $(\sigma_1' + \sigma_2')/2$
q	Shear stress, $(\sigma_1 - \sigma_2)/2$
S	Undrained Strength Ratio
S_i	Initial Saturation
q_f/σ_{vc}'	Undrained Strength Ratio
S_u/σ_{vc}'	Undrained Strength Ratio
S_u	Undrained shear strength
σ_{vc}'	Vertical Consolidation Effective Stress
σ_v'	Vertical Effective Stress
σ_h'	Horizontal Effective Stress
σ_1'	Major Principal Effective Stress
σ_3'	Minor Principal Effective Stress
t_p	Time to end of primary
Δu	Excess pore pressure
Δu_s	Shear-induced pore pressure
w	Water content
w_L	Liquid Limit
w_p	Plasticity Index

1.0 INTRODUCTION

1.1 Background and Problem Statement

A very popular framework for the estimation of the undrained shear strength of clays, for use in design, is called the SHANSEP[1] method (Ladd & Foott, 1974). This method describes how the undrained shear strength of soil can be evaluated based on the stress history profile of the deposit in conjunction with the appropriate NSP[2].

Currently, there are three methods to evaluate the undrained shear strength of cohesive soils: (1) the SHANSEP method, (2) direct field measurement which includes the FV test (Field Vane), (3) the Recompression method which involves consolidating an inherently disturbed soil sample past its in situ vertical effective stress and performing undrained shearing; this method is performed using both the UU test (Unconsolidated Undrained shear test) and the U test (Unconfined Compression Shear Test).

The SHANSEP method to evaluate the undrained shear strength was developed because the authors thought that the existing methods, the field testing and the recompression method, were either highly empirical or yielded such uncertain results that they gave the engineer little control over his design.

SHANSEP is based on the concept of normalized soil behaviour, which is founded on the concept that mechanical properties are proportional to consolidation stress. This is the basis of CAM CLAY (Schofield, Roscoe &Wroth, 1958 and Roscoe & Burland, 1968), "simple" clay (Ladd, 1960) and some advanced analytical models such as MIT-E3 (Whittle and Kavvadas, 1994). In addition, SHANSEP includes a prescriptive method to consolidate the sample in the laboratory.

In this thesis, it was described how the basis for this school of thought was derived from research carried out on the effects of sample disturbance, strength and stress-strain anisotropy, strain-rate effects as well as normalized soil behaviour on undrained

[1] SHANSEP – Stress History And Normalized Soil Engineering Properties
[2] NSP – Normalized Soil Parameters

shear strength. The following paragraphs will describe each of these effects on the undrained shear strength in more detail.

When a sample is removed from the ground, it undergoes a significant amount of disturbance. Studies on sample disturbance have been carried out by a number of authors including Poulos and Davis (1967) et al. As the sample is removed from the ground it experiences both vertical and horizontal stress relief. Since the sample is contained within a capped tube upon removal, and swelling is not allowed, negative pore pressures develop within the sample. Sampling leads to decrease in the effective stress of the sample. In order to establish some way of evaluating the degree of sample disturbance, Ladd and Lambe (1968), compared the negative pore water pressures within several disturbed samples with the pore pressures that would occur in a "perfect" sample. What they found, was that the pore pressures in the "perfect" sample were typically 20±20% greater than the pore pressures measured in the disturbed sample which translates into a relative decrease in effective strength between the "perfect" sample and the undisturbed sample. Upon performing UU tests on "perfect" samples and comparing the S_u values to tests performed on tube samples (which are inherently undisturbed), they found that the S_u values were 20% - 50% higher than that of the tube samples. The "perfect" sample is one that "only" experiences the stress relief effect of the sampling process; other disturbance processes are unimportant.

Strength anisotropy was first considered theoretically by Hansen and Gibson (1948). However, it was only until work done in the 1960's, through attempts to compare S_u values derived using different types of shear tests, was the theory recognized as having practical significance.

There are two types of strength anisotropy; the first, an inherent anisotropy, is due simply to the naturally occurring orientation of the soil particles within the soil fabric. The second, which Ladd and Foot (1974) referred to as stress induced anisotropy, occurs as a result of changing the direction of the principal stresses during shear stress application. This is demonstrated by illustrating the direction of the principal stresses on samples in situ in typical construction situations. This is shown in Figure 1:1 along with the shear tests that would most accurately represent the given scenario.

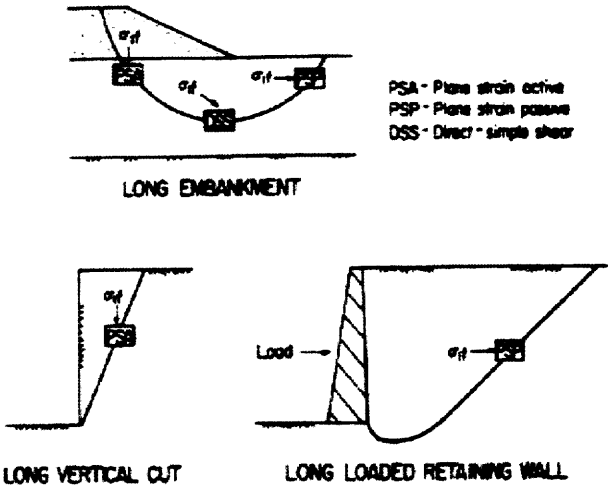

Figure 1:1 An Illustration Showing the Orientation of the Principal Stresses in Typical Construction Situations

The findings of this study on homogenous non-layered clays suggested that the S_u values obtained from PSA tests is greater than those obtained from the DSS tests, which is greater than those obtained from the PSP tests. It should be noted that TE strengths are very close to PSA strengths and that TE strengths are roughly 10%-25% less than strengths obtained from the PSP tests.

Previous works done by Bjerrum et al have indicated that the strain rate at which a test is performed, affects the undrained shear strength value obtained from the test. The finding of this work surmises that a log cycle decrease strain rate corresponds to a 10±5% decrease in S_u. Ladd and Foot (1974) go on to explain that the main reason that this occurs due to undrained creep, which occurs during shear in the sample, resulting in increased pore pressures, decreased effective stress and decreased strengths.

A reason was offered that explained why these more traditional methods of measuring the undrained shear strength have worked in past design practice; the methods tended to be self-compensating. So for instance, the increased Su values obtained from the high strain rate tests, such as U and UU, are compensated for by the lowering of the Su values caused by sample disturbance. However, it can clearly be seen that this is random and the engineer has little control over the design. As a result, it was a

feasible endeavour to explore another method for estimating the undrained shear strength.

At the root of the SHANSEP method, is the concept of normalized soil behaviour. Extensive research at both Imperial College, London, England and MIT has shown that the stress-strain characteristics of clays with the same OCR, normalized with respect to vertical consolidation stresses, are very similar, regardless of the maximum past pressures (σ'_{vm}) of the clay (Ladd & Foott, 1974). This normalization concept is illustrated in Figure 1:2 below.

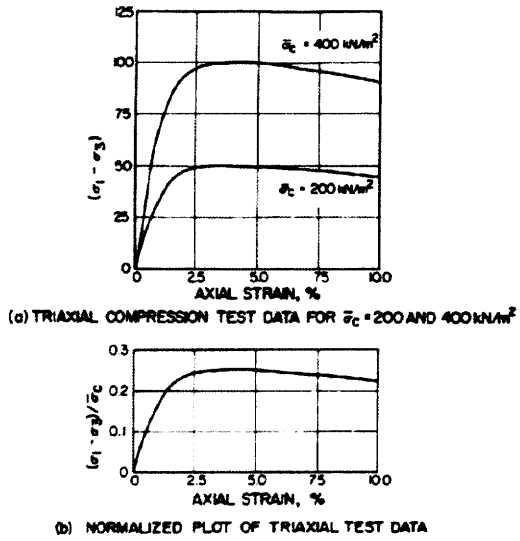

Figure 1:2 Example of Normalized Behaviours Using Idealized Triaxial Compression Test Data for Homogenous Normally Consolidated Clay

For normally consolidated soils, the concept of normalized behaviour can be described by two principles as shown in Figure 1:3 below (Ladd 2000, MIT 1.361 class notes). Principle I illustrates a unique failure envelope and Principle II describes a unique relationship between w_f, q_f, and p_f, that is parallel to the virgin compression line (VCL).

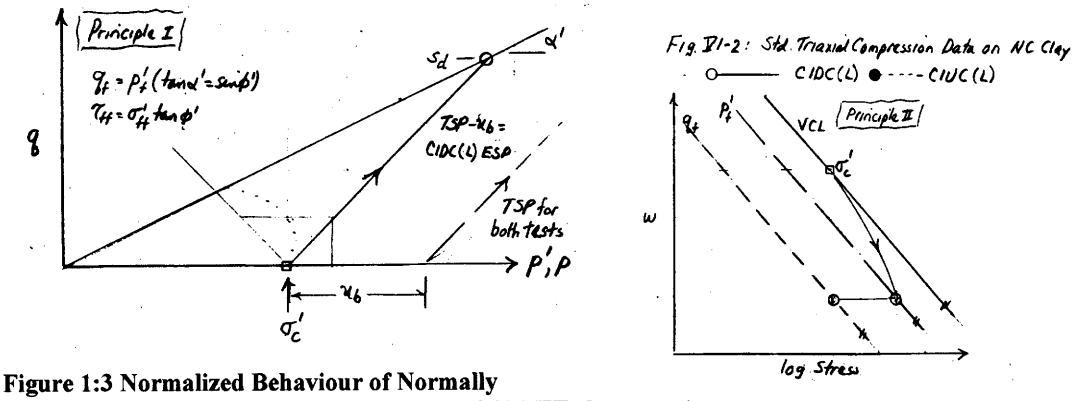

Figure 1:3 Normalized Behaviour of Normally Consolidated Clays (OCR=1) (Ladd 2000, 1.361 MIT class notes)

The preceding discussed the normalized behaviour on normally consolidated soils (OCR=1). The SHANSEP equation was developed to describe the normalized behaviour of over consolidated soils. The SHANSEP relationship is given by the following equation: $(S_u/\sigma'_{vc}) = S(OCR)^m$. The parameters 'S' and 'm' are derived after carrying out several shear strength tests with varying vertical consolidation stresses and plotting the relationship between the undrained shear strength ratio (S_u/σ'_{vc}) and the over consolidation ratio on log-log axes. The 'S' parameter is the undrained shear strength ratio when the soil is normally consolidated. The 'm' parameter is the slope of the line. This relationship can be developed using different types of shear strength tests (TC, DSS or TE) and the appropriate shear strength can be selected for design depending on the nature of the foundation problem. This is illustrated in Figure 1:4 below.

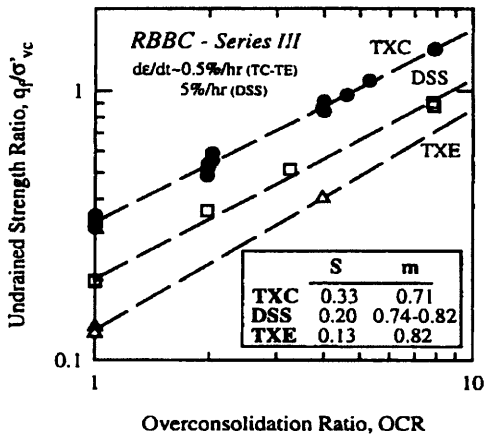

Figure 1:4 Undrained strength ratio versus OCR from CK0U test in triaxial compression (Sinfield 1994, Santagata 1994), extension (Sheahan 1991), and direct simple shear (Ahmed,1990). Resedimented Boston Blue Clay

In order to successfully apply the SHANSEP method to provide reliable evaluation of design parameters, the following steps must be carried out:

- Establish stress history, i.e., the profile of σ'_{v0} and σ'_{p}, which determines the range of OCR values for which data are required.
- Perform a series of CK0 shear tests, with representative modes of failure, on specimens consolidated beyond the in situ preconsolidation pressures (to σ'_{vc} greater than 1.5 to 2.0 times the σ'_{p}) to measure the behaviour of normally consolidated clay and also on specimens rebounded to varying OCR to measure overconsolidation behaviour.
- Express the results in terms of NSP and establish NSP versus OCR relationships, i.e., c_u/ σ'_{vc} versus OCR (the resulting relationship can be expressed as, $c_u/ \sigma'_{vc} = S\ (OCR)^m$; where $S= c_u/ \sigma'_{vc}$ for normally consolidated soil)
- Use these NSP relationships and the stress history information to compute a profile of cu, etc.

(Ahmad 1990 & Jamiolkowski et al 1985)

Ladd and Foot (1974) go on to describe the limitations of and expected variations within the normalized soil parameters concept. Normalized behaviour is not as perfect as is illustrated in Figure 1:2. Variations in peak strength may be due simply to variations in test procedures, the vertical consolidation effective stress or properties of the soil, such as, initial water content. However, it was then concluded that for all practical purposes that the NSP concept could be applied to a wide range of soils because the aforementioned variations only result is a small divergence (±10%) from the mean measured strengths. It should also be mentioned that quick clays and naturally cemented clays do not exhibit normalized behaviour due to the inherent soil structure which is destroyed during consolidation. Another major limitation is that the deposits must have a fairly well defined stress history and high quality samples must be used for testing.

Currently, at MIT, research is being conducted on wellbore stability in strong soils (Abdulhadi, 2009). This involves undrained triaxial compression testing on RBBC at high confining stress levels $\sigma'_v \leq 100$ ksc (10.0 MPa). Historically, research done on undrained triaxial compression tests at MIT, was carried out at vertical confining pressures $\sigma'_v \leq 80$ ksc (0.8 MPa). To date the findings of this research has suggested that at confining stresses greater than $\sigma'_v \leq 10$ ksc (1.0 MPa), it is clearly established that strength varies with the consolidation effective stress level, $\sigma'_{v;}$ the concept of normalized soil behaviour is no longer applicable. Undrained triaxial compression tests on RBBC have shown that the soil stiffness and strength is dependant on the vertical consolidation effective stress and that the strength behaviour does not strictly conform to a normalized framework. This is contradictory to the normalized soil behaviour previously described. These findings are illustrated graphically in Figure 1:5 and Figure 1:6.

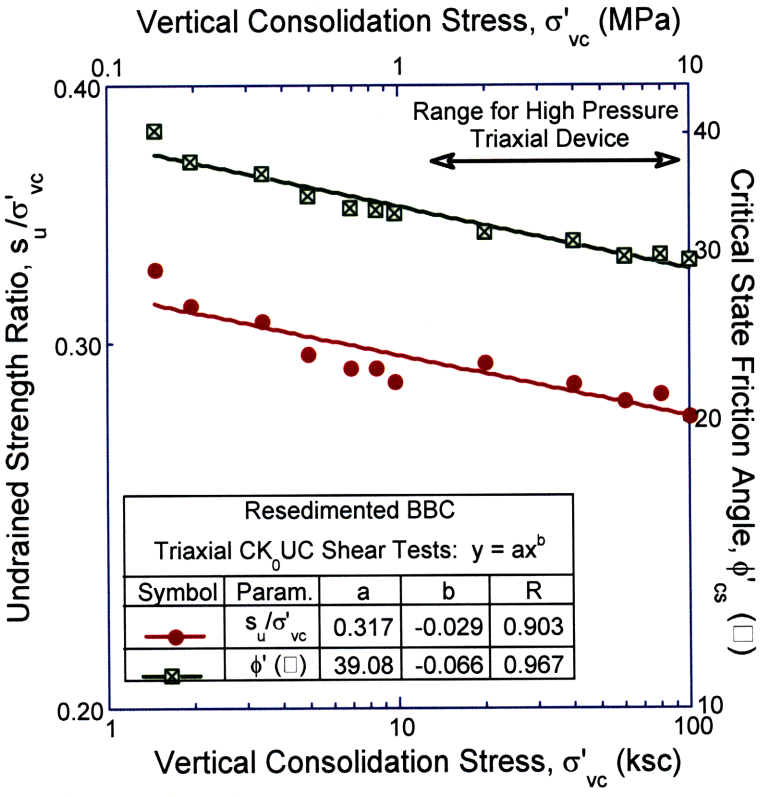

Figure 1:5 Undrained strength ratio and critical state friction angle of K_0-normally consolidated RBBC as a function of the consolidation vertical effective stress (Abdulhadi, 2009)

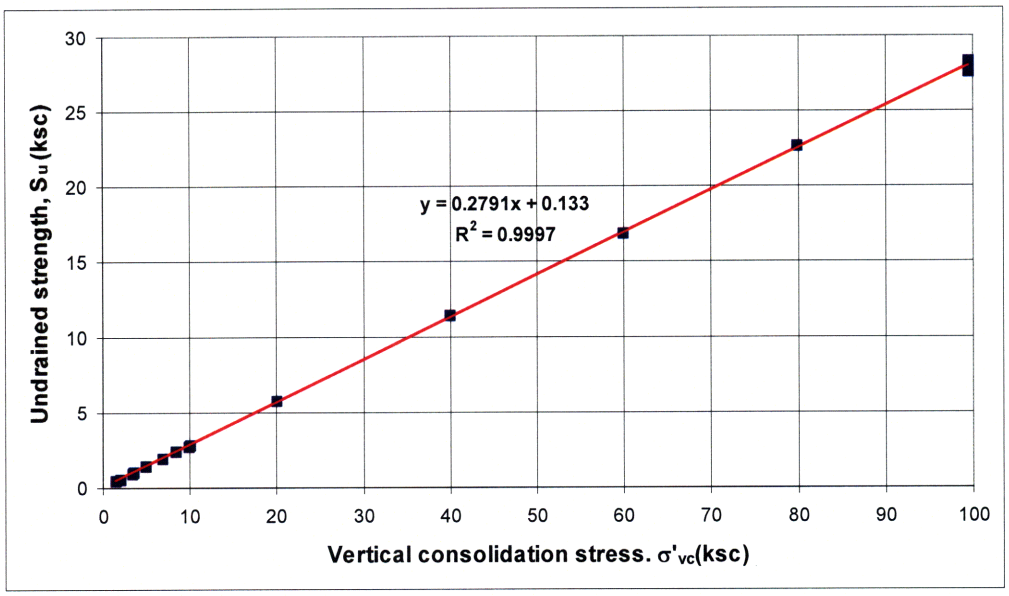

Figure 1:6 Undrained shear strength of K_0-normally consolidated RBBC as a function of the consolidation vertical effective stress (Abdulhadi, 2009)

1.2 Objectives of Research

The aim of this study is to explore the relationship between vertical consolidation stress and the undrained shear strength behaviour in extension for cohesive soils to determine whether the normalized soil parameter concept (and hence SHANSEP) is still applicable at vertical consolidation stresses ranges of $\sigma'_v \geq 1.0$MPa.

In order to investigate this, a series of K_0 consolidated undrained triaxial extension tests (CK_0UE) were carried out over a range of vertical consolidation effective pressures ($\sigma'_v \leq 2.0$MPa) as the basis for this investigation.

The material that was used for testing was Resedimented Boston Blue Clay (RBBC). Each sample was made by mixing powdered BBC into a slurry mixture. The slurry was then poured into a consolidometer and allowed to consolidate to 0.1MPa (1.0 ksc). The sample was then unloaded to an OCR =4, extruded from the consolidation tube and placed in the triaxial machine. More detail will be provided on the specimen preparation and test procedure in the following sections. The specimen was then K_0 consolidated to vertical effective stresses of 0.15 MPa, 0.2MPa, 0.4MPa, 1.0MPa and 2.0MPa in the triaxial cell. Finally, it is sheared in extension under undrained conditions.

1.3 Thesis Organization

Chapter 2 of this thesis describes the material used for this study. The mechanical and index properties from previous research and will be reviewed. The reason that RBBC was selected will also be discussed.

Chapter 3 outlines in detail the procedure used to prepare the samples as well as the procedure of the CK_0UE test. Any equipment used to carry out the study will be identified in this section as well.

Chapter 4 consists of the results obtained from the laboratory tests. The results of the strength data obtained and the consolidation data acquired during the batching process is presented. This chapter also discusses the results presented in comparison to existing data obtained from previous works. This chapter also comments on the relationship between vertical consolidation stress and the undrained shear strength behaviour in extension for cohesive soils to determine whether the normalized soil parameter concept (and hence SHANSEP) is still applicable at vertical consolidation stresses ranges of $\sigma'_v \geq 1.0$MPa.

Chapter 5 concludes the findings of the study and suggests future research for this are of study.

2.0 TEST MATERIAL AND GENERAL CHARACTERISTICS

This chapter describes the material used for this study. The mechanical and index properties from previous research will be reviewed. The reason that RBBC was selected will also be discussed.

2.1 Resedimented Boston Blue Clay – Origin

This chapter provides a summarized description of both the origin and properties of Resedimented Boston Blue Clay (RBBC); the material that was used to carry out this study. RBBC is a soil resedimented from natural Boston Blue Clay, an illitic CL consisting of glacial outwash deposited in a marine environment 14000 to 12000 years ago, in the period immediately following the Wisconsin deglaciation of the Boston basin (Kenny, 1964).

The primary reason that RBBC has been used for this study, and in general as a standard test material at MIT, is that BBC samples that have been produced from the well established resedimentation process (Germaine, 1982) yield very similar mechanical, engineering and index properties making it an ideal testing material for investigating soil behaviour. Further, RBBC exhibits characteristics very similar to those of the original material, and to many natural cohesive soils, including stress-strain-strength anisotropy, low to medium sensitivity, and significant strain rate dependency (Santagata, 1999). The well defined and repeatable behaviour of RBBC has also made it an asset in the development and proofing of new laboratory apparatuses as well as the modification or automation of existing devices (Santagata, 1999). In addition, BBC can be found in abundance throughout the Boston area.

The material used in this testing program was obtained in 1992 from the base of an excavation for MIT's Biology Building (Building #68) at a depth of about 12m; where the soils have an OCR ranging between 1.3 to 3.4 (Berman 1993). This batch of BBC is referred to as Series IV, indicative of the fourth location from which BBC has been retrieved since it was first used at MIT.

2.2 Resedimented Boston Blue Clay – Processing and Sample Batching

The following describes the process by which the natural material is prepared for testing. This procedure was adapted from Santagata (1999) and Abdulhadi (2009).

After the BBC material is removed from the ground, it was mixed with tap water and blended into a thick slurry. The slurry was then passed through a #10 US standard sieve to remove all non-soil material, gravel, coarse sand, and large shell fragments and oven dried at 60^{o} C in preparation for grinding. The dried material was ground to 95% passing a #100 US sieve using a roller mill. Finally, the material was manually randomized by two blending operations. The dry powdered form of BBC is then stored in sealed 40 gallon containers for subsequent use.

To make a single sample, appropriate for one triaxial specimen, the following procedure was followed. This procedure was also adapted from Abdulhadi (2009).

A one to one mixture consisting of 500 g of powdered BBC and 500 g of water is mixed together for approximately 20 mins until a homogenous mixture with no visible lumps was attained. Sodium chloride was added to the mixture at a concentration of 6 g/kg of soil-water mixture, in order to achieve a flocculated particle structure and to prevent a dispersed structure from forming during sedimentation.

The slurry mixture is then vacuumed to remove as many entrapped air bubbles as possible. After vacuuming, the de-aired soil is poured into a 2.5 in (63.5 mm) diameter consolidometer. The inside of the consolidometer is greased with silicon oil to minimize wall friction during consolidation as well as to ease the sample extrusion process. Porous stones and filter paper are placed both at the top and bottom of the soil samples to facilitate drainage during consolidation.

Once poured into the consolidometer, the sample is then loaded incrementally, with a LIR = 1, starting with a vertical effective stress of 0.03 ksc (0.003 MPa) to a maximum vertical effective stress of 1.0 ksc (0.1 MPa) then subsequently unloaded to achieve an OCR of 4. At OCR=4 the soil is close ot hydrostatic conditions (i.e., K_0 is

near unity) and the shear strains due to the removal of the soil cake from the consolidometer are minimal, as confirmed by the work performed by Santagata (1994) on sample disturbance. Hence, RBBC batches have essentially no sample disturbance (Santagata, 1999).

Each load increment is left for 24 hrs which is past the primary consolidation time for each load increment. The maximum stress is held for at least one cycle of secondary compression. During each load increment, the vertical deformation of the sample is recorded with an LVDT. A photo of the consolidometer with the LVDT setup is shown below in Photo 1 below. A typical relationship between the vertical displacement during the sedimentation process and time is shown in Figure 2:1 below. This figure shows that the time for primary compression for this load increment is approximately 16.7 hrs.

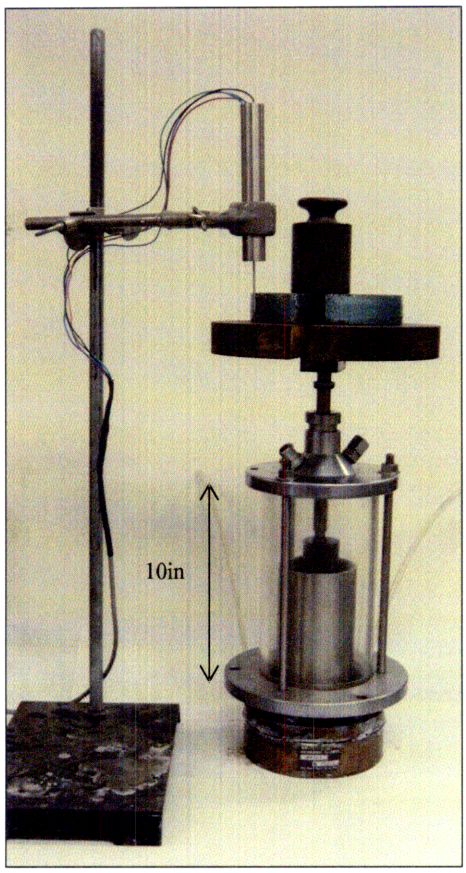

Photo 1 Consolidometer Setup with LVDT

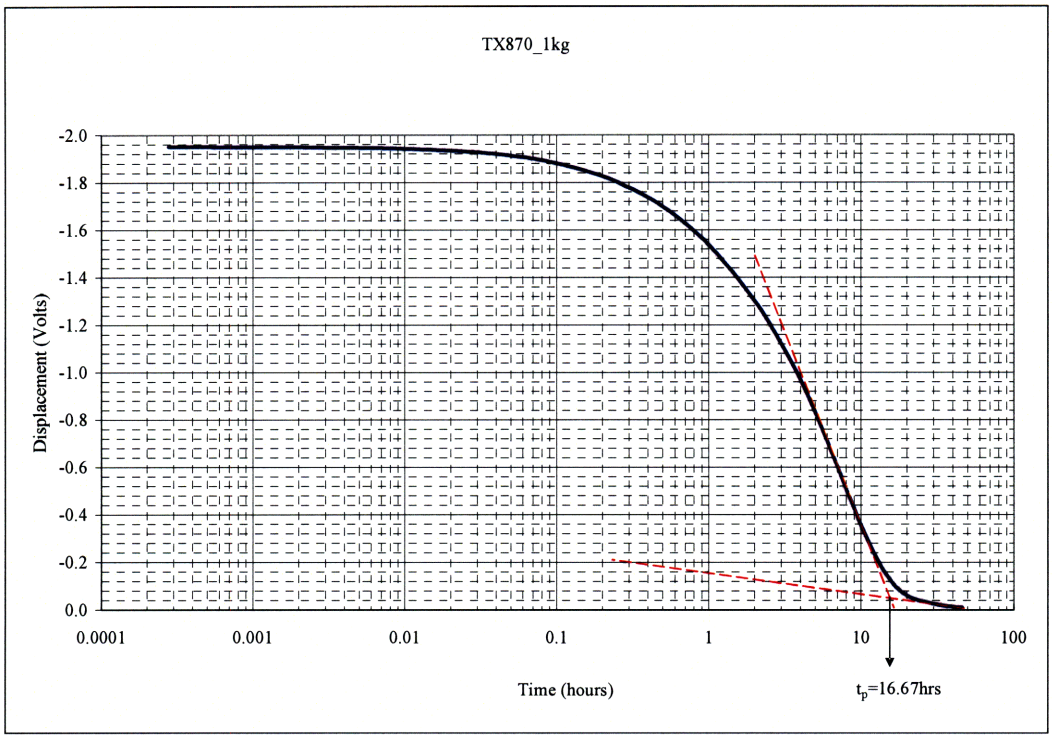

Figure 2:1 Typical Displacement - Time Relationship for One Load Increment

Table 2:1 below shows a summary of all the tests carried out as a part of this study and the vertical effective stress levels at which each test was carried out.

	Test Number	Batch Maximum Consolidation Stress (σ'_{vc})		Time at Maximum Load	Vertical Consolidation Effective Stress (σ'_{vc})	
		(ksc)	(MPa)	(days)	(ksc)	(MPa)
1	TX870	1.0	0.1	2	1.5	0.15
2	TX872	1.0	0.1	2	10.0	1.0
3	TX875	1.0	0.1	2	20.0	2.0
4	TX883	1.0	0.1	2	20.0	2.0
5	TX899	1.0	0.1	2	2.0	0.2
6	TX903	1.0	0.1	2	2.0	0.2
7	TX904	1.0	0.1	2	4.0	0.4
8	TX909	1.0	0.1	4	20.0	2.0

Table 2:1 Summary of all the CK_0UE Tests carried out

After the sample is loaded to OCR=4, it is then extruded from the consolidometer and sample is then trimmed to a diameter of approximately 35mm (1.4 in) and prepared

for testing. A description of the triaxial testing procedure used in this study is presented in Chapter 3.

2.3 Resedimented Boston Blue Clay – Index Properties

The index properties for RBBC Series IV have been extensively investigated by several authors including Sinfield (1998), Cauble (1996), and Santagata (1998). The following test results are the record of index tests carried out by Abdulhadi (2009).

The grainsize distribution for Series IV RBBC is shown in Figure 2:2. The distribution shows that the soil has a fine fraction (% passing the #200) greater than 98% and an average clay fraction (% less than 2 μm) of 56%. These values are reasonably consistent with those obtained from previous studies.

The Atterberg Limits tests carried on the current Series IV RBBC show that the average plastic limit, w_p= 23.5± 1.1%, liquid limit, w_L= 46.5±0.9% and plasticity index, Ip= 27.7±1.2%. These results are also consistent with results obtained from previous studies. The plasticity chart showing these results is presented in Figure 2:3 on the next page, confirming that BBC is classified as a CL soil.

The measurements of specific gravity G_s, for Series IV RBBC yielded an average value of 2.81, which is slightly higher than previous research, but is within expected range of illitic clays (G_s = 2.60 for illites; Lambe and Whitman 1968).

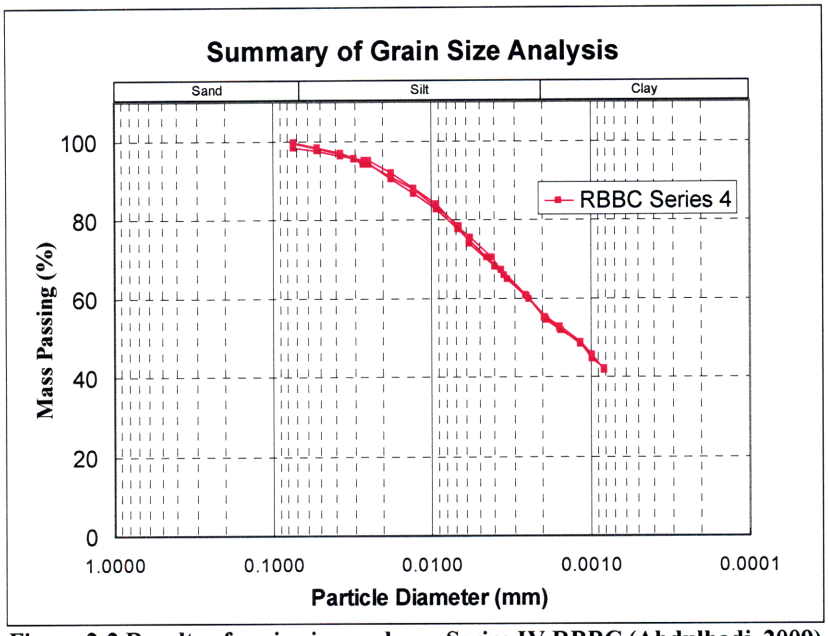

Figure 2:2 Results of grain size analyses, Series IV RBBC (Abdulhadi, 2009)

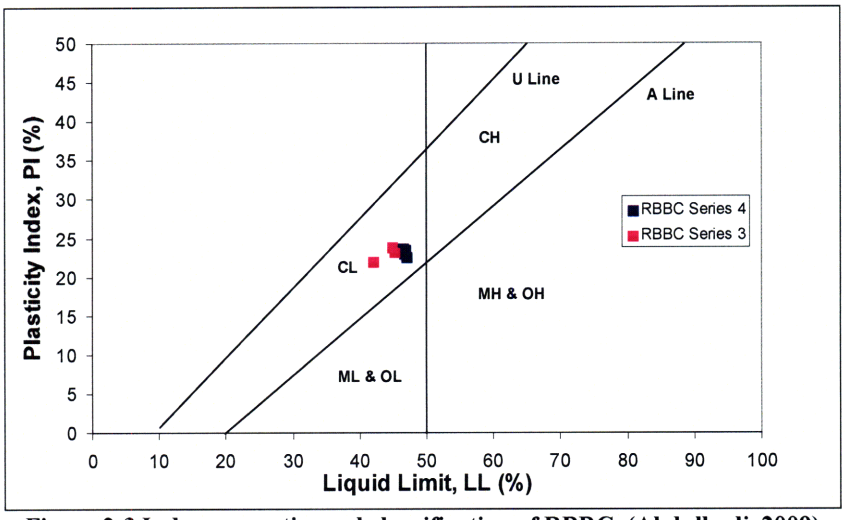

Figure 2:3 Index properties and classification of RBBC (Abdulhadi, 2009)

2.4 Resedimented Boston Blue Clay – Mechanical Properties

The section serves to summarize the mechanical properties of BBC. The typical compression behaviour along with the shear strength – strain behaviour is obtained from undrained triaxial extension tests will be discussed.

Consolidation Behaviour

The compression behaviour of Series IV RBBC can be derived from both the CRS (Constant Rate of Strain) test as well as the 1-D consolidation phase of triaxial tests. These results were taken from Abdulhadi (2009) and are presented in Figure 2:5 and Figure 2:4 below. In both data sets the samples were consolidated to vertical consolidation effective stress of 100ksc (10MPa). Also in both cases a maximum past pressure (σ'_{vm}) of 1.0ksc is apparent; indicative of the maximum past pressure that the soil was subjected to in the laboratory during sample preparation.

The CRS test was performed by vertically loading the sample at a rate of 2%/hr. The data presented in Figure 2:4 shows that the consolidation line is not linear in the e-logσ'_v space. The compression index C_c ($=\Delta e/\Delta \log \sigma'_v$) ranges from 0.39 to 0.28.

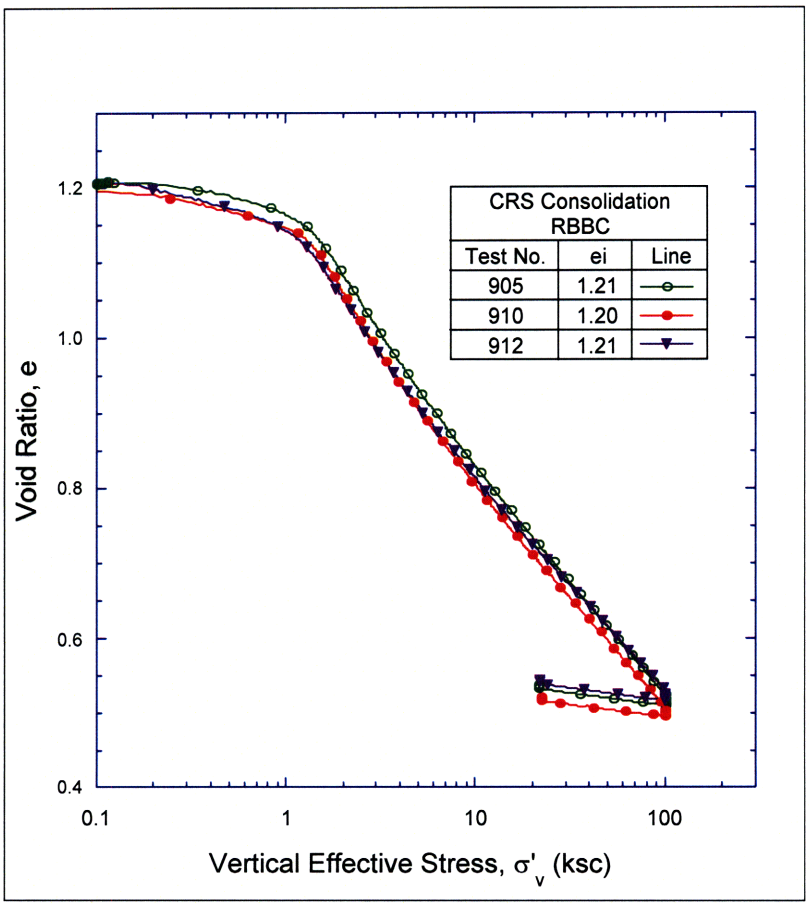

Figure 2:4 Compression behaviour of Series IV RBBC from CRS 1-D consolidation tests (Abdulhadi, 2009)

The 1-D consolidation data presented in Figure 2:5 was derived from vertically loading the sample at a rate of 0.15%/hr during the consolidation phase of the triaxial test.

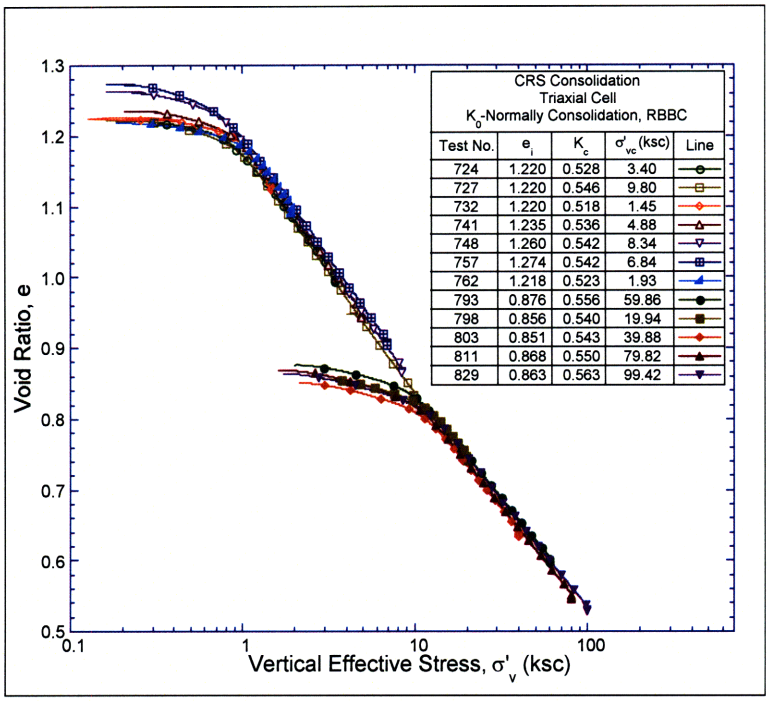

Figure 2:5 Compression behaviour for Series IV RBBC measured in 1-D consolidation phases in triaxial cells (Abdulhadi, 2009)

Figure 2:6 shows the variation in the coefficient of consolidation with vertical effective stress. This shows that below the maximum past pressure (σ'_{vm}) the values of c_v decrease with increasing vertical effective stress. After this stress they increase to a maximum value ranging from 30 to 50 x 10^{-4} cm^2/sec. These data are also consistent with data obtained from previous consolidation tests on Series III BBC (Sheah,1989).

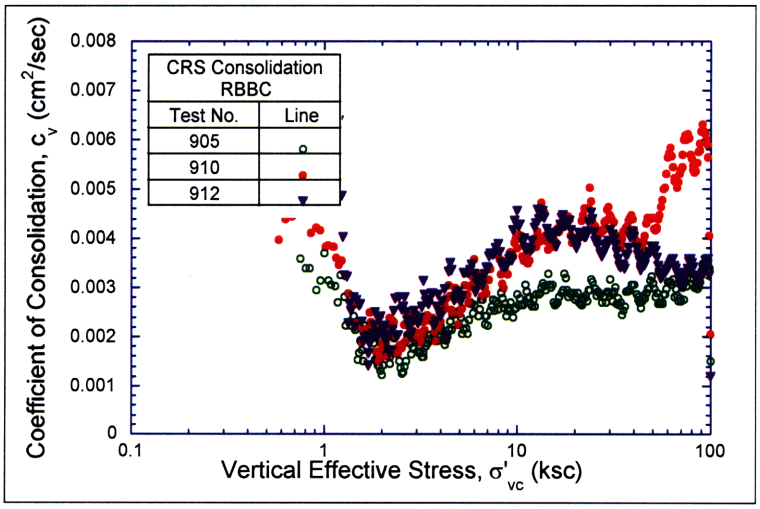

Figure 2:6 Vertical consolidation coefficient (c_v) from 1D CRS tests on Series IV RBBC (Abdulhadi,2009)

Vertical hydraulic conductivity measurements were also taken for the CRS tests shown in Figure 2:4. These results show that the hydraulic conductivity decreases with decreasing void ratio and increasing vertical stress. (See Figure 2:7 below).

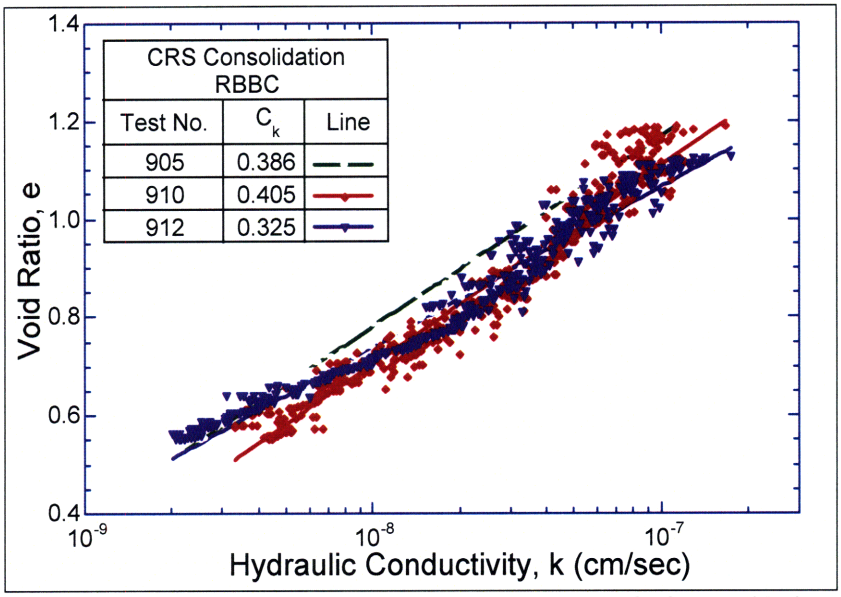

Figure 2:7 Hydraulic conductivity for Series IV RBBC measured in CRS consolidation tests (Abdulhadi, 2009)

The relationship between the vertical consolidation stress (σ'_{vc}) and the lateral earth pressure coefficient K_0 is shown in Figure 2:8 below. This shows that K_0 decreases during the recompression phase of consolidation and then plateaus to a steady state value until the desired vertical consolidation stress is reached.

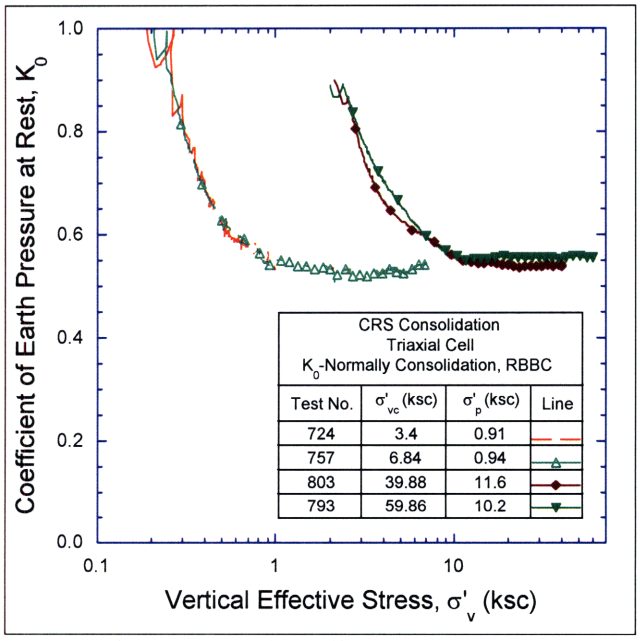

Figure 2:8 Lateral stress ratio versus vertical effective stress (σ'_{vc}) during K_0-consolidation of RBBC (Abdulhadi, 2009)

In the following Figure 2:9, the shear stress paths during undrained compression, for ten K_0 normally consolidated RBBC samples, is shown. Each sample was consolidated to a different stress level between 1.5 – 100ksc at a strain rate of 0.5%/hr.

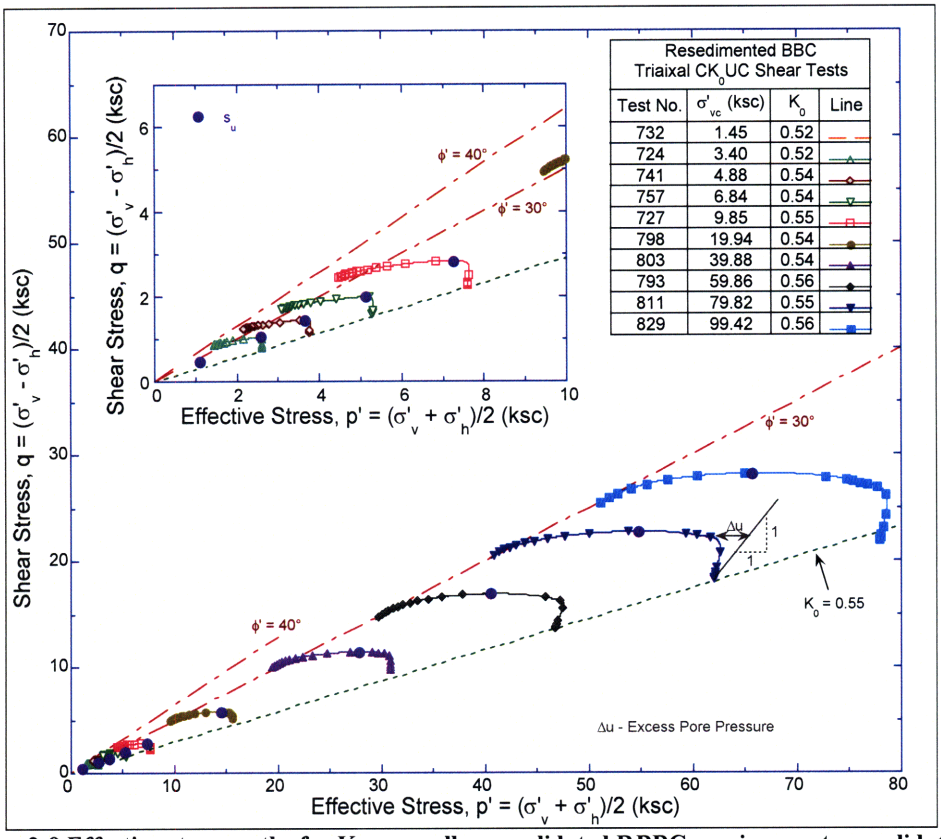

Figure 2:9 Effective stress paths for K_0-normally consolidated RBBC specimens at consolidation stresses σ'_{vc} = 1.5 – 100 ksc

3.0 EQUIPMENT AND PROCEDURES

3.1 Introduction

This chapter outlines the procedure used to prepare the samples as well as the procedure of the CK_0UE test. Any equipment used to carry out the study will be identified in this section as well.

3.2 Triaxial Equipment

The first automated triaxial equipment was developed by Sheahan in 1991 at the MIT geotechnical laboratory as a part of the FATCAT (Flexible Automation Technology for Computer-Assisted Testing) system. Since then the process has been improved and modified by the introduction of adaptable automation (Sheahan and Germaine, 1992) where each component is modified to permit automation. A complete description of the automated triaxial equipment can be found in Sheahan (1991) and Sheahan and Germaine (1992). A schematic representation of the automated triaxial equipment is illustrated in Figure 3:1 below.

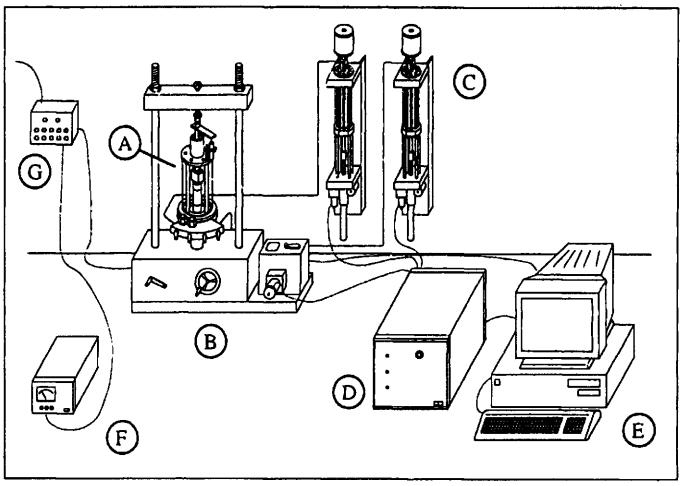

A - Triaxial Cell
B - Load Frame
C - Pressure/Volume Controllers
D - Motor Control Box
E - Personal Computer
F - DC Power Supply
G - Data Acquisition Channels

Figure 3:1 MIT Automated Stress Path Triaxial Cell - Schematic (connections between transducers and PC not shown) (Santagata 1994)

The following is a description of the triaxial machine as well as the triaxial testing procedure used to carry out the tests for this study, was taken and adapted from Mazzei (2008).

The machine that was used to carry out the testing for this study was comprised of Wykeham Farrance bench top load frame from the 1960's retrofitted with an electric servo motor. The triaxial cell is composed of a Wykeham Farrance base from the 1960's with customized features such as linear ball-bearing bushings for alignment and an o-ring seal with an internal load cell to eliminate piston friction, a fixed top cap for testing on clay, top and bottom drainage, ball valves, copper tubing and silicone oil as cell pressure fluid to eliminate the problem of leakage through the membrane. The pore and cell pressure transducers are connected directly to the triaxial base so as to reduce the system compliance. Pressure/volume actuators, equipped with DC electric servo motors, maintain the pore and the cell pressure. These two motors, as well as the motor driving the load frame, are controlled by the MIT designed motor control box. The automated control is performed by a program written in BASIC and running on a personal computer. The program is able to perform all phases of a triaxial test including initial pressure up, back pressure saturation, B-value check, consolidation along any specified stress path or K_0 consolidation, and shear in extension or compression. Much of the hardware has been developed in the MIT geotechnical laboratory, including the 22-bit analog to digital integration card. More recently, the triaxial cells have been modified to accommodate electronics within the pressure chamber. Cells used for this research are available to test at pressures as high as 2.0 MPa. The current systems include internal force transducers to measure the deviator force applied to the specimen. The following table, Table 3:1, shows the transducers used to collect the data and the calibration factor associated with each one.

Transducer	Calibration Factor
Pore Pressure	701.62 ksc/v/v
Cell Pressure	-698.6 ksc/v/v
Load Cell	6714 kg/v/v
Axial DCDT	2.481 cm/v/v
Volumetric DCDT	23.848 cc/v/v

Table 3:1 Calibration Factors of Transducers Used for the Testing

3.3 Triaxial Test Procedure

Consolidation and Sample Preparation

After the RBBC specimen is prepared according to Section 2.2, it is then extruded from the consolidometer and trimmed to the desired cross sectional area of approximately 35mm (1.4 in) using a wire saw for the rough trimming and a razor blade for the final trimming. The ends of the specimen are also cut off to the desired height. The height of the sample was determined, based on the recorded strains during the test, as well as, the limitation of the piston height of the triaxial machine. The trimmings and the cut ends are collected and the moisture content is determined. After trimming to the desired size, the initial specimen wet mass is taken along with several measurements of the specimen diameter and height are taken using vernier calipers. The averages of each of these dimensions are used as input values during the testing phase. At the end of the test, the dry mass of the specimen is measured and used to calculate the initial void ratio, saturation and total density. After the specimen is trimmed and the mass and dimensions are recorded, it is put aside while the triaxial machine is prepared for testing.

Triaxial Setup

The standard MIT procedure was used for the initial setup of each test. The first step in preparing the triaxial equipment is to perform thorough leak checks to make sure there is no loss in cell or pore pressures during the test. If this happens, the data obtained from the test would be incorrect.

Before the test is started; it is necessary that the zero values were taken for each of the five transducers; the load cell, the cell pressure, the pore pressure, the displacement LVDT, and the volume LVDT. These values are input into the computer as the reference values for all measurements taken during the test. To take the zero value of the load cell, the load cell was connected and allowed to come to a steady value. This was done just after the o-rings and the membranes were placed onto the base, and before the specimen was placed into the machine. The zero value for the pore pressure transducer was also taken at this time. The zero value for the cell pressure was taken when the cell was half way filled with silicone oil. The zero value for the Axial

LVDT was taken after the displacement transducer was set up, and firmly connected to the piston. Finally, the volume zero value was taken at the end of the setup process.

During the test measurements are recorded by the transducers and stored on the in house central data acquisition system.

Once the machine is checked for leaks, cleaned and it is ensured that all the o-ring seals are tight, the next step is to place the specimen into the machine. The sample is carefully placed into the machine on the base pedestal squarely under the top cap. Two pieces of filter and two porous stones are placed at the top and bottom of the sample to allow for drainage during the consolidation phase of the test.

After the sample is in place two thin membranes are then rolled over the sample and greased o-rings are used to hold them in place during the test. The plexiglass cell is placed over the sample, closed and then filled with silicone oil.

Pressure Up

The purpose of this stage is to measure the sampling effective stress of the specimen. The cell pressure was increased to 30% of the vertical effective stress with the pore pressure valves closed; this is enough to cause a positive pore pressure value. The specimen was allowed to equilibriate overnight at this pressure and the following day the sampling effective stress and the axial strain recorded. This effective stress will be maintained during the back pressure saturation portion of the test.

Back Pressure Saturation and B-Value check

The sample is then back pressure saturated maintaining the sampling effective stress measured in the pressure up part of the test. This is done by hydrostatically loading the specimen so that any air voids in the specimen or equipment is compressed and dissolved into solution.

To ensure that the sample and the equipment are fully saturated, a B-value check was carried out after back pressure saturation. The B-value is an empirical parameter developed by Skempton (1954) to evaluate the way the pore pressure responds to

stresses. The B-value is given by the relationship $\Delta u/\Delta\sigma_3$=B. A B-value of unity signifies that an increase in cell pressure corresponds to an increase in pore pressure and the sample is fully saturated. To measure the B-value, pore pressure valves are closed and a cell pressure increment of 25kPa (0.25ksc) is applied and the pore pressure response is monitored. If the resulting B-value is over 0.95, the test is continued. If not the back pressure saturation is continued until a value of at least 0.95 is obtained.

K_0 Consolidation

After the specimen and equipment is fully saturated and a B-value of unity, or an acceptably high value (B > 0.95), is obtained, the next phase of the test involves consolidating the sample to a desired vertical effective stress. For this study, the effect of vertical effective stress level was the manipulated variable so each test was consolidated to a different level of stress. Table 2:1 shows the vertical effective consolidation stress level of each test.

K_0 is defined as the lateral earth pressure coefficient at rest and is the ratio of horizontal effective stress to vertical effective stress when lateral strains are zero.

K_0 consolidation is performed in the triaxial tests by using a combination of three feedback loops: back pressure is held constant; axial strain at specified rate; and cell pressure is adjusted so that volumetric strain is held equal to the axial strain. The axial strain rate is set at 0.15% per hour in all tests.

Secondary Compression

When the sample reaches the desired axial consolidation stress level, this stress level is maintained for a period of 24 hours. During secondary compression, the axial strain increases due to creep while the axial stress is held constant. The relationship between strain and time during secondary compression is a soil property that can be described as:

$$C_\alpha = d\varepsilon_a / d \log(t - t_p)$$

Where $d\varepsilon_a$ is the change in strain, t is time and t_p is the time to the end of primary compression.

Shear

After consolidating to the desired axial effective consolidation stress, the sample is ready to be failed in undrained shearing. To achieve undrained conditions, the pore pressure valves must be closed during shearing. Before shearing the pore pressures should be monitored for about 30 mins to ensure that there are no leaks or pore pressure loss. During the shear phase of the test the sample is failed by decreasing the axial stress at a rate of 0.5 %/hr while holding the confining stress constant. During shearing the shear stress of the sample increases to a maximum value; this value is taken as the undrained shear strength, S_u, of the soil. In triaxial extension tests, this maximum value is typically attained after undergoing at least 14% strain. As such, the samples were all sheared to more than 15% strain or when a failure plane was apparent. After testing the sample is removed from the machine and the wet and dry masses are recorded. The data are retrieved from the data acquisition system and is converted to engineering values.

Data Reduction

To covert the data collected from the transducers and stored on the data acquisition system, a BASIC program called "MIT Triaxial Reduction Data Editor Revision 1.1" was used. A summary of the options chosen within the program, to reduce the data, is as follows:

- Type of Test: Consolidation or Undrained Shear (depending on the stage of the test being reduced)
- Membrane Correction: 2 Thin Membranes
- Area Correction: Right Cylinder
- Filter Strip Correction: No
- Internal Strain Measurements: No
- The normalized zero values taken from the voltmeter are used as the zero values in the reduction file.
- The shear data were normalized to the average vertical consolidation stress attained between the end of primary consolidation and the end of the 24 hr period of secondary consolidation.

Additional Data Analysis Comments

Consolidation Data:

During initial hydrostatic consolidation, the volumetric strains are assumed to be equal to the axial strains. Therfore, the initial volumetric strains must be equal to the initial axial strains. As such, after the consolidation data is reduced using the BASIC program, a quick arithmetic calculation must be carried out to find out the new zero value for the volumetric strain that will make it equal to the axial strain. This new volumetric zero value is then input into the reduction file and the data is re-reduced.

Shear Data:

The initial portion of the stress-strain curve is used to calculate the modulus of the soil. However, the very beginning of this plot is usually a curved line due to mechanical backlash problems; these few data points do not represent the modulus of the soil.

To get a better representation of the modulus, the straight line portion of the stress strain curve is extrapolated such that, there is a straight line from zero strain. To achieve that a new initial point must be selected. This initial point is then put into the data file (*.DAT file) and the data is subsequently, re-reduced. The resulting stress strain plot should have an initial straight line portion. Another check would be that when the modulus was plotted against strain on a log-log plot, the initial part of the curve is a straight line parallel to the x-axis.

4.0 TEST RESULTS & DISCUSSION

4.1 Introduction

A total of eight specimens were prepared for CK_0UE (K_0 Consolidated Undrained Extension) testing as a part of this study. The following table shows data that were successfully collected from each test. The table presented below, Table 4:1, provides a list of the tests done and a description of the data collected from the tests. Consolidation data were successfully obtained from 7 out of 8 of the tests and shear data were collected from 4 out of the 8 tests. A tabulated summary of both the consolidation and shear test data is presented in Appendix I.

	Test Number	Consolidation Data	Shear Data	Remarks
1	TX870	✓	✓	Specimen length was too long for the machine to perform 15% strain. The peak strength was not reached during shear. However, the data quality collected from both phases of the test is good.
2	TX872	✓	✓	Good data collected during both the consolidation and shear phases of the test.
3	TX875	✓	×	Relay switch malfunctioned during the "hold stress" stage (secondary compression) after the end of primary consolidation. The consolidation data is good.
4	TX883	✓	×	Relay switch malfunctioned during the "pressure up" stage (secondary compression) after the end of primary consolidation. The consolidation data is good.
5	TX899	×	×	Relay switch malfunctioned during the "pressure up" stage (secondary compression) after the end of primary consolidation. Data from this test was not of good quality.
6	TX903	✓	×	Errors in the program, caused fluctuation during the "hold stress" stage (secondary compression) after the end of primary consolidation. The consolidation data is good.
7	TX904	✓	✓	Good data collected during both the consolidation and shear phases of the test.
8	TX909	✓	✓	Good data collected during both the consolidation and shear phases of the test.

Table 4:1 Data Collected from Each Test

4.2 Consolidation Test Results

Vertical Strain and Effective Stress

Figure 4:1 shows the relationship between vertical strain (ε_a) and the consolidation effective stress (σ'_v). This relationship shows the consistency in the consolidation behaviour of RBBC. From the chart below, it is evident that the maximum past pressure or the preconsolidation pressures (σ'_{vm}) in each of the specimens is approximately 1.0 ksc. This is consistent with the maximum stress that the specimen was consolidated to in the laboratory during specimen preparation.

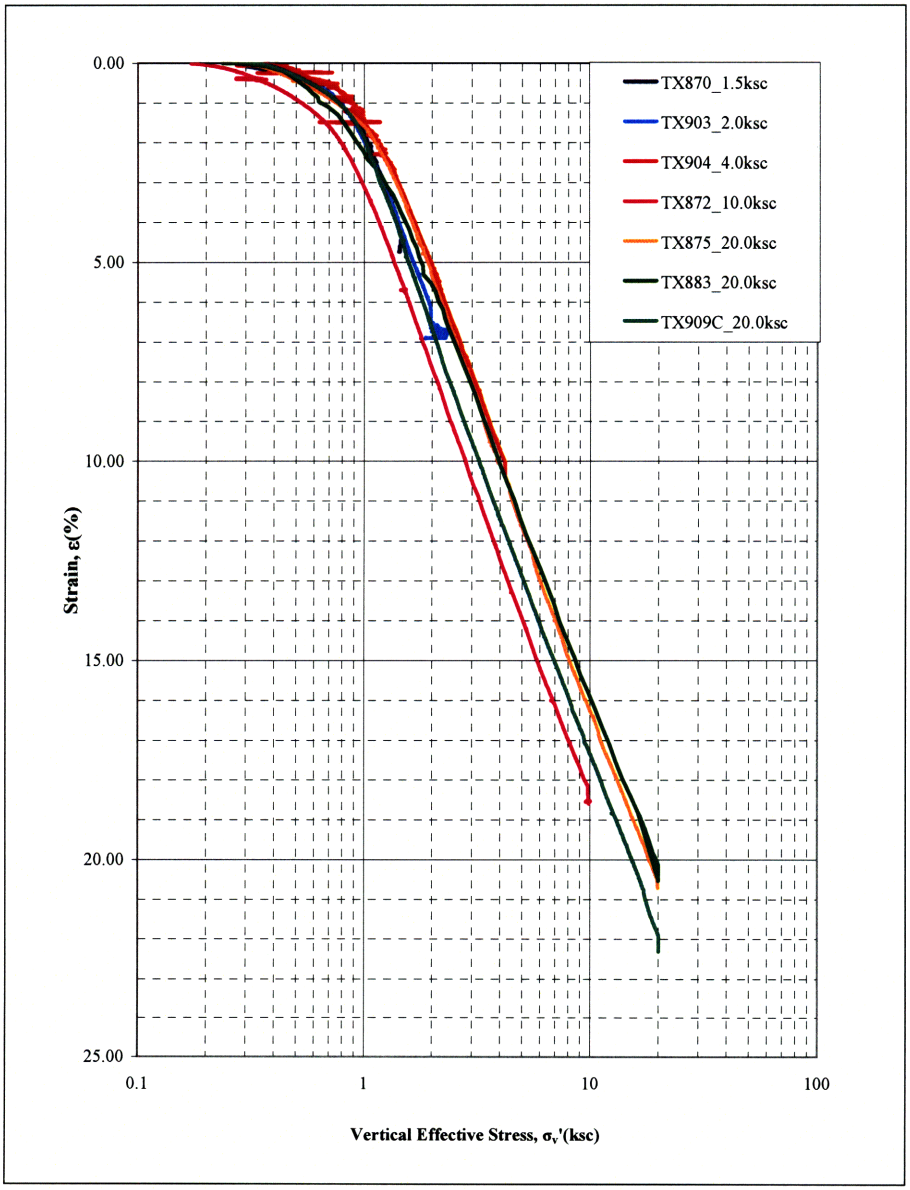

Figure 4:1 Strain (ε_a%) vs Vertical Consolidation Effective Stress (σ'_v)

Work and Effective Stress

The following figures, (Figure 4:2 and Figure 4:3), show the relationship between work and vertical effective stress. The main reason that the consolidation data is plotted in terms of work and effective stress is that it is the best way of determining the preconsolidation pressure (σ'_{vm}). This is called the Strain Energy method (Becker et al., 1967); where the work per unit volume for 1-D consolidation tests is plotted against effective vertical consolidation stress. The preconsolidation pressure is determined by constructing two lines on each straight portion of the curve; the point on the x-axis corresponding to the intersection of these construction lines is taken as the presconsolidaion pressure. Figure 4:3 shows a magnification of the area demarcated with the red dashed box in Figure 4:2. This portion of the plot was magnified to improve the scale where the curve transition occurs.

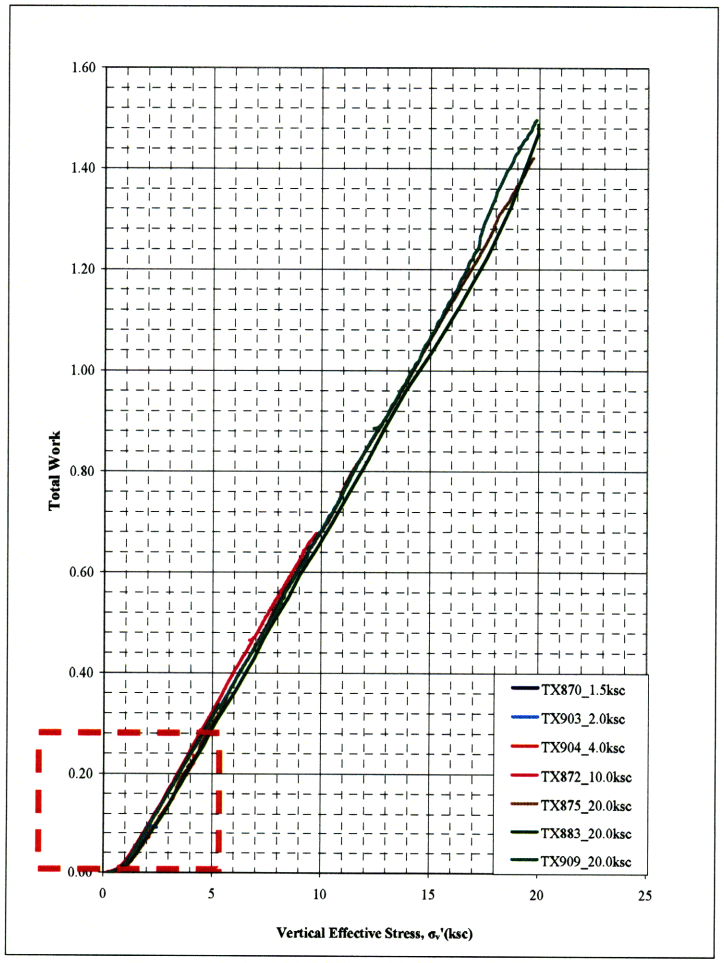

Figure 4:2 Work vs Vertical Effective Stress (σ'_v)

Figure 4:3 below shows a magnification of the area demarcated with the red dashed box in Figure 4:2 above. The x-coordinate of the intersection point of the two straightline portions of each series, is taken as the preconsolidation pressure (σ'_{vm}). The preconsolidation pressures measured from this plot ranged from 0.85 ksc to 1.15 ksc.

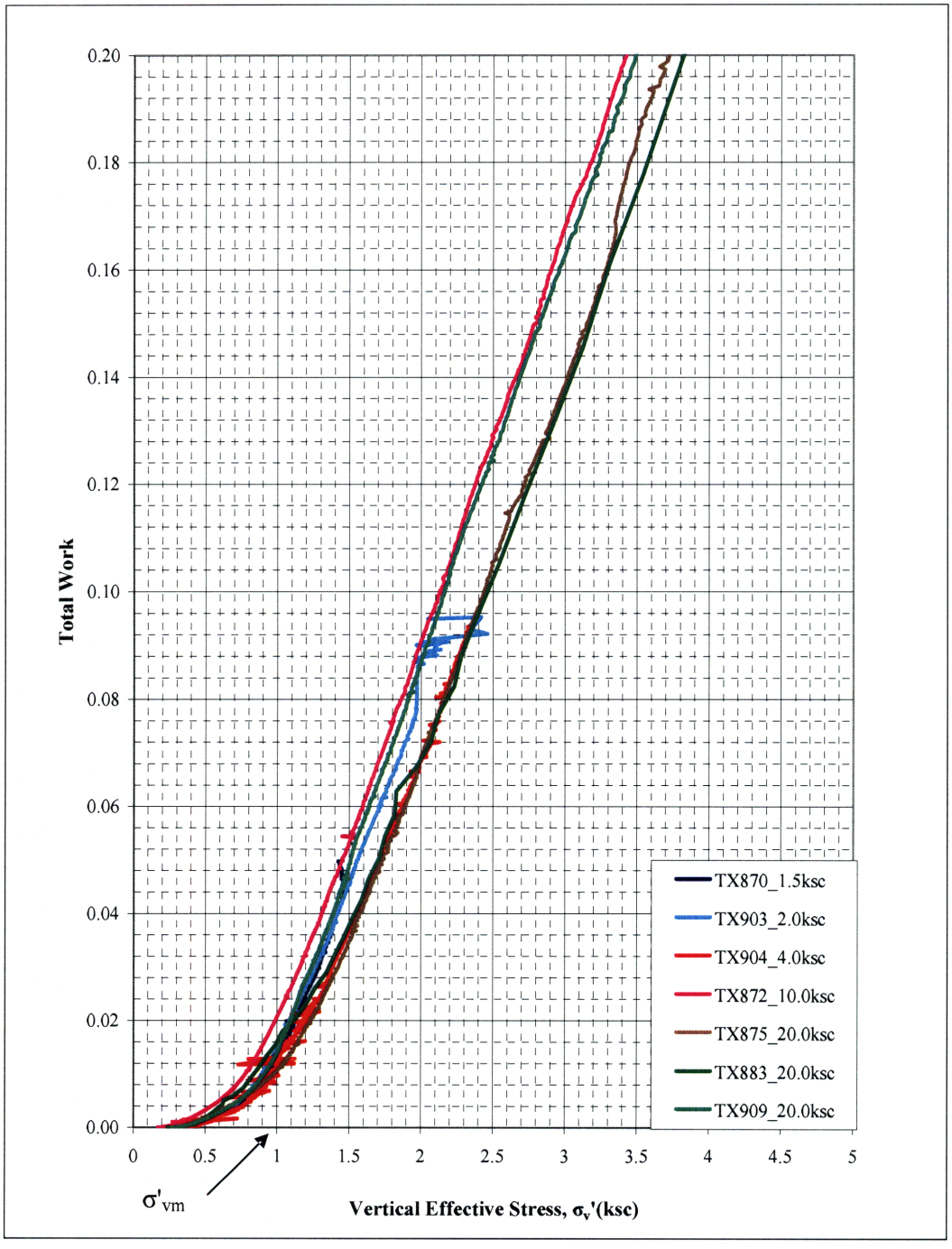

Figure 4:3 Work vs Vertical Effective Stress (σ'_v)

Void Ratio and Effective Stress

The following figure (Figure 4:4) shows the relationship between void ratio (e) and the consolidation effective stress (σ'_v). The initial void ratios range from 1.16 to 1.24 at the start of the consolidation portion of the tests for five of the seven consolidation test results. This is fairly consistent with the initial void ratios, 0.86 to 1.22, obtained from the consolidation portion of the CK_0UC and CRS tests carried out by Abdulhadi (2009). (See Figure 2:4 and Figure 2:5).

The compression index C_c ($=\Delta e/\Delta \log \sigma'_v$) values obtained from these tests range from 0.34 to 0.42. On average, these values are slightly higher than the C_c values (0.28 to 0.39) obtained from the consolidation portion of the CK_0UC and CRS tests carried out by Abdulhadi (2009). (See Figure 2:4 and Figure 2:5).

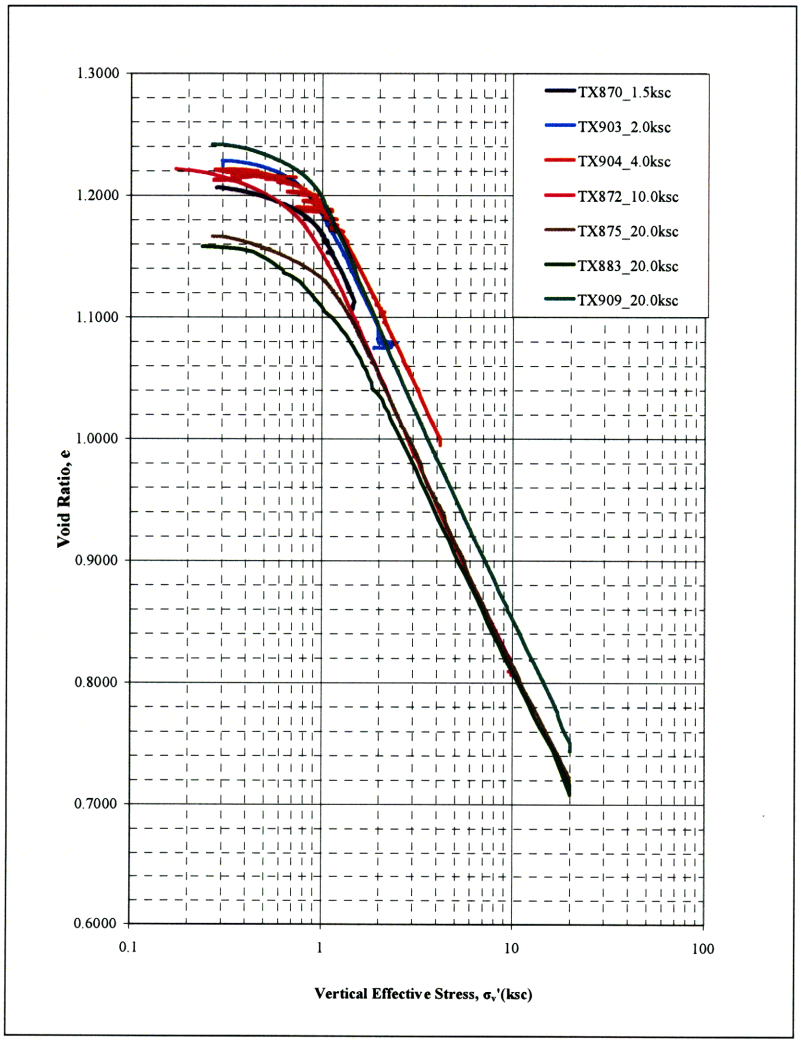

Figure 4:4 Void Ratio (e) vs Vertical Effective Stress (σ'_v)

Lateral Stress Ratio and Effective Stress

Figure 4:5 shows the variation of the lateral stress ratio (K_0) with vertical effective stress (σ'_v). The beginning of all tests started with hydrostatic conditions, i.e. the horizontal effective stresses (σ'_3) and the vertical effective stresses (σ'_1) are equal. Thus the lateral stress ratio (K_0), which is the ratio of these two stresses, starts at about unity. As the specimen approaches the preconsolidation pressure, the values of K_0 reach a minimum and then increase slightly to a steady state value. This behaviour is typical of Series IV RBBC as shown in Figure 2:8 Lateral stress ratio versus vertical effective stress (σ'vc) during K0-consolidation of RBBC (Abdulhadi, 2009).

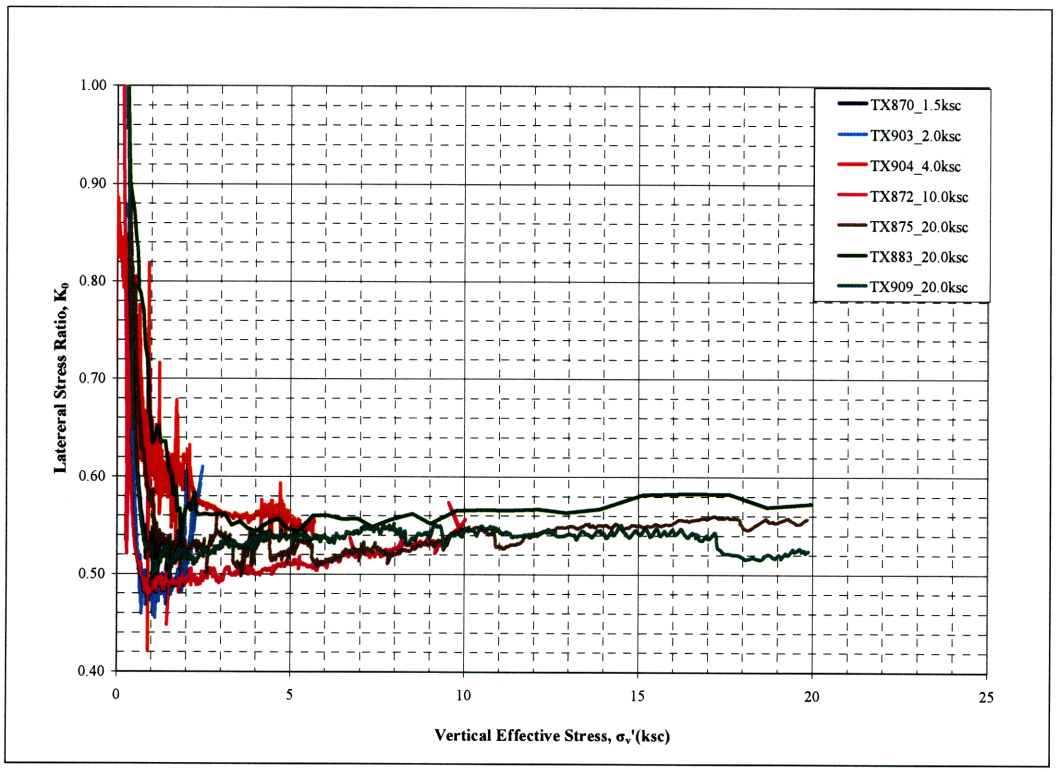

Figure 4:5 Lateral Stress Ratio (K_0) vs Vertical Effective Stress (σ'_v)

4.3 Shear Test Results

After the specimen has been K_0 consolidated to the desired vertical effective stress level, the specimen is then sheared in extension; the axial stress is decreased by extending the specimen at a constant rate of deformation while the radial or confining stress is held constant. The following sub-sections show the different measurements taken during the test and an interpretation of the results. As mentioned in Table 4:1, shear data was successfully attained from four of the tests.

Shear Strength

The following figures (Figure 4:6 and Figure 4:7) show the relationship between the normalized shear stress (q_f/σ'_{vc}) and axial strain ($\varepsilon\%$). These plots show that after an axial strain of only 0.5%, the shear stress reaches the hydrostatic axis; the shear strength goes to zero. It is also of note that very large axial strains (~14 %) are required to mobilized the peak shear strength as compared to compression tests where as little as 1 % strain.

From Figure 4:6 it can be seen that the peak shear strength is attained only after 14 % strain. This value of peak shear strength (q_f) is also the undrained shear strength value (S_u). The variation in normalized undrained shear strength with vertical stress level is shown clearly in Figure 4:7.

After an axial strain of 14%, where the peak strength occurs, the specimen has undergone so much deformation, that the end of the stress – strain curve becomes erratic (See Figure 4:6). At this point a fully developed failure plane can be seen on the specimen. During the test it was observed that a neck occurs in the sample before a failure plane is developed. A photograph of the failure plane and the neck observed before failure is presented in Figure 4:6. To the right of the photo, a schematic of the expected failure mechanism of failure during shearing in extension is shown. Both the photo and the schematic are presented in Figure 4:8 below.

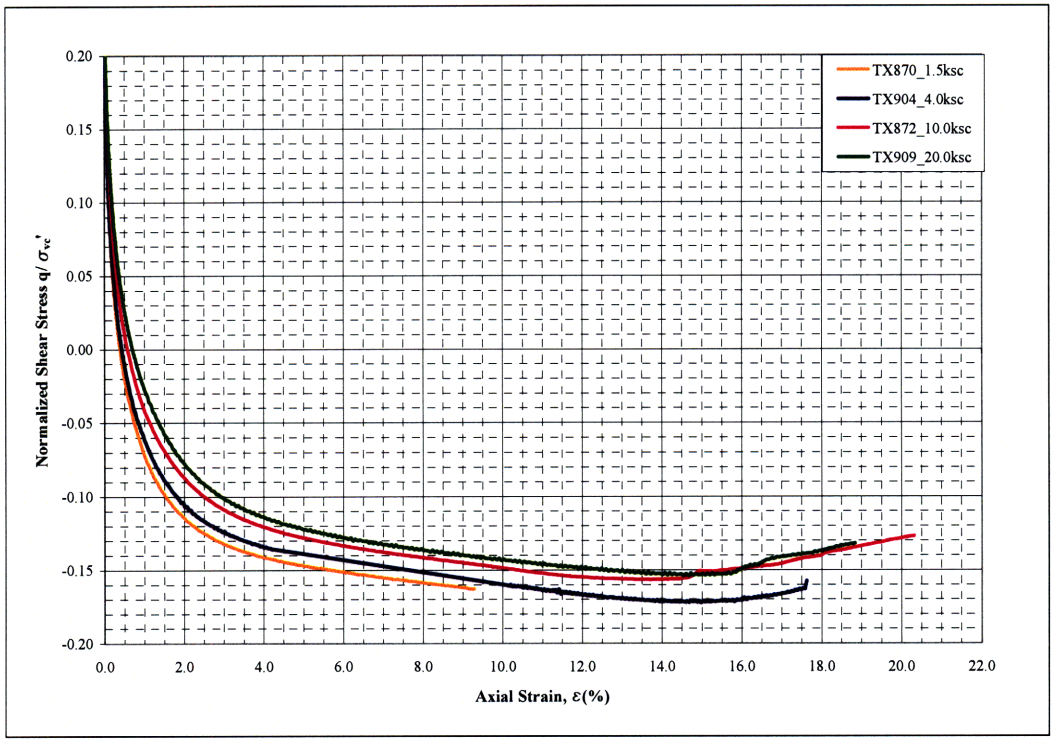

Figure 4:6 Normalized Shear Strength (q_f/σ'_{vc}) vs Axial Strain (ε%) to Failure

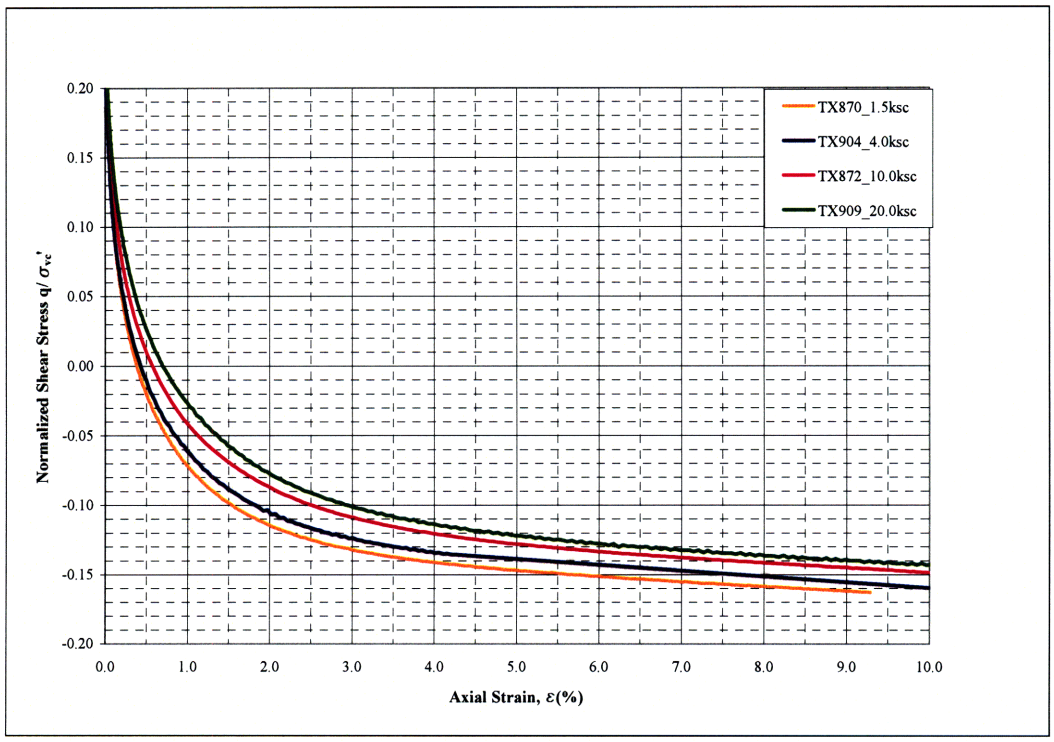

Figure 4:7 Normalized Shear Strength (q_f/σ'_{vc}) vs Axial Strain (ε%) to 10% Strain

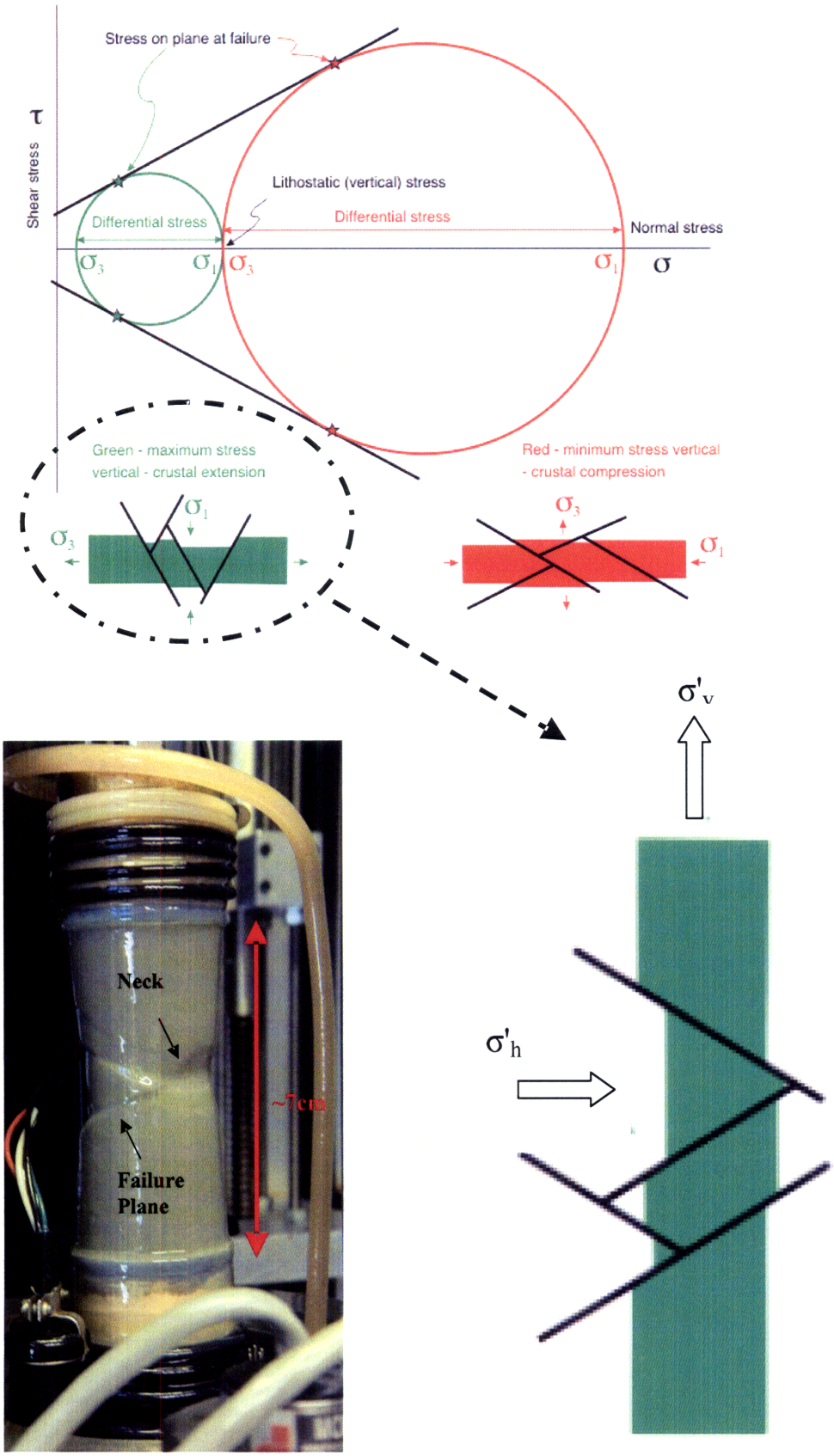

Figure 4:8 Photo and Schematic of the Necking and Failure Plane During Extension. (Schematic taken from http://courses.eas.ualberta.ca/eas421/diagramspublic/Mohrstressdiag.gif)

To clearly show the variation in the normalized shear stress level (q/σ'_{vc}) with vertical effective stress level, the absolute values of the shear stress levels at various strains (attained from Figure 4:7), were plotted on Figure 4:9 below. The normalized peak shear strength (also called the undrained shear strength ratio, (S_u/σ'_{vc}), was also plotted on this chart. Logarithmic equations best fitting the data have also been presented.

There is a very clear trend that can be observed from Figure 4:9; the undrained shear stress level, and consequently, the undrained shear strength, decreases with vertical effective stress.

The undrained shear strength ratio at a vertical consolidation stress of 4.0 ksc appears to be slightly higher than expected based on the other three trendlines. The variation in undrained shear strength with vertical consolidation stress is also shown in Figure 4:10 below.

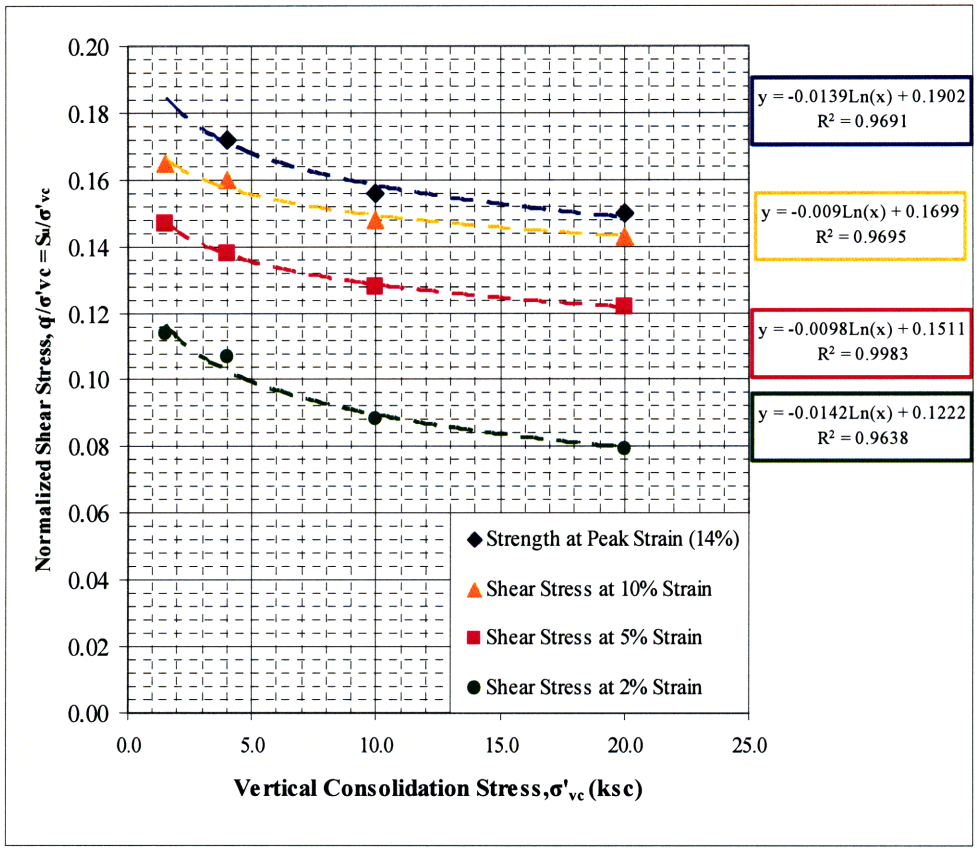

Figure 4:9 Variation of Normalized Shear Stress (S_u/σ'_{vc})with Vertical Effective Stress (σ'_{vc}) for different levels of strain

Figure 4:10 below shows the variation in shear strain, and undrained shear strength, S_u, with vertical consolidation effective stress. The slope of the trends vary from 0.075 to 0.144. In each trendline there is a small intercept ranging from 0.06 to 0.11 ksc (5.9 to 10.8kPa). Linear equations representing the shear stress level with vertical consolidation stress, at a given strain, are also presented below.

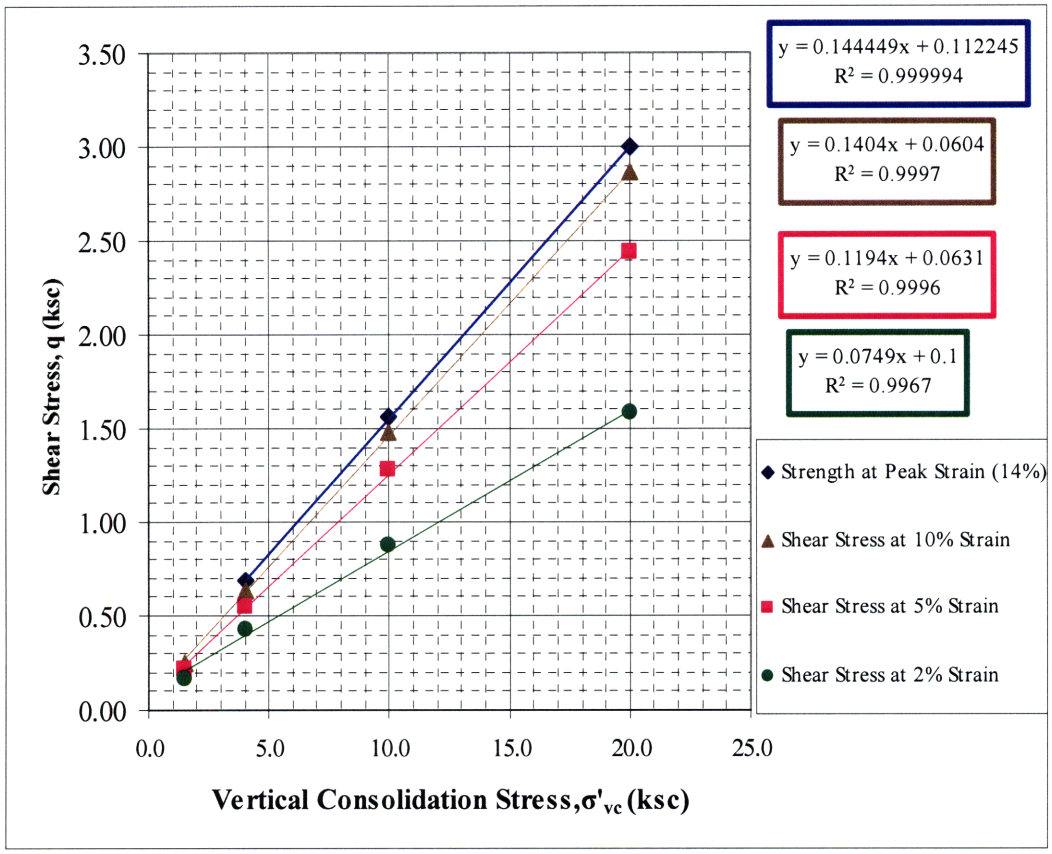

Figure 4:10 Shear Stress Level (q) vs Vertical Consolidation Stress (σ'_{vc})

The figure below, Figure 4:11, shows the variation of the undrained shear strength ratio, (S_u/σ'_{vc}), with vertical consolidation effective stress (σ'_{vc}) for both compression and extension shear. The shear strength data from the extension tests was obtained from tests done as a part of this study; it is the shear strength data presented in Figure 4:9. The shear strength data from the compression tests was taken from Abdulhadi (2009), where CK_0UC tests were performed on Series IV RBBC. This figure shows clearly the anisotropy associated with shear strength in compression and extension. Using these results, the shear strength in compression is 1.74 to 1.90 times greater than the shear strength obtained from the extension tests.

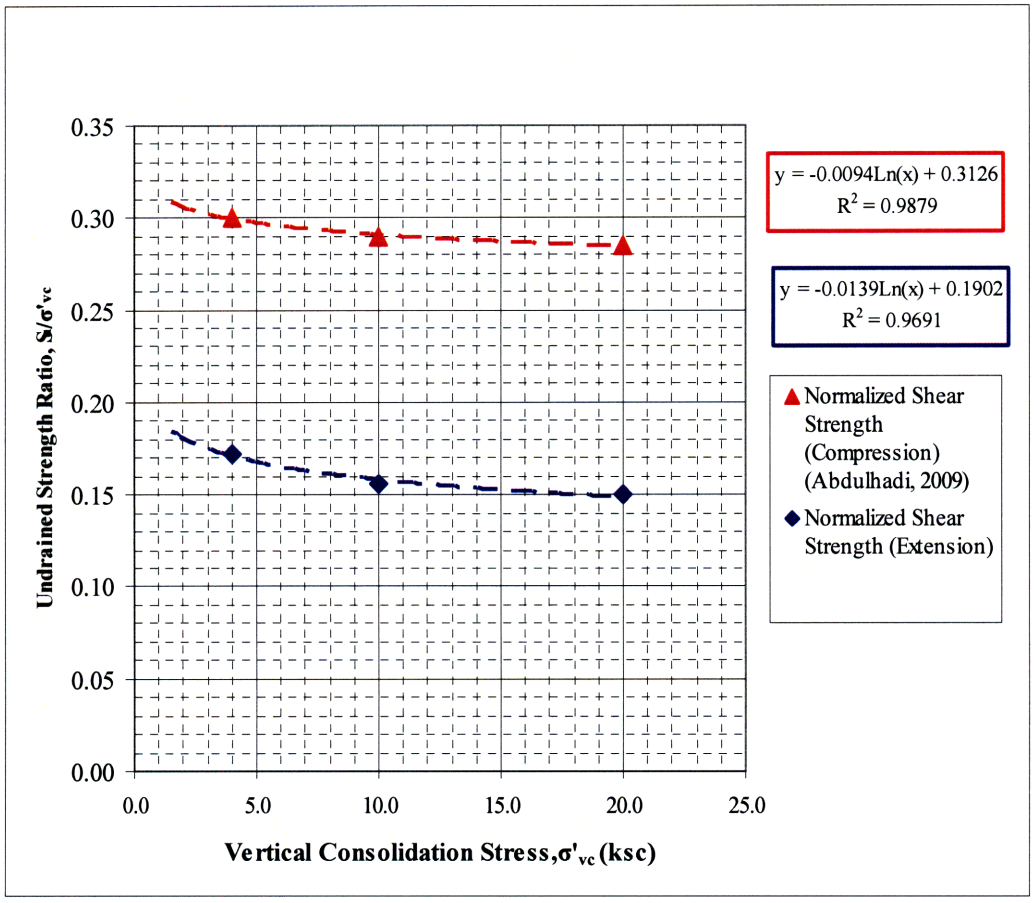

Figure 4:11 Undrained Strength Ratio (S_u/σ'_{vc}) vs Vertical Consolidation Stress (σ'_{vc}) - Anisotropy in Compression and Extension

Secant Modulus and Axial Strain

The variation in the normalized secant modulus with axial strain is shown in Figure 4:12. This figure shows that upon yielding, which occurs at approximately 0.05% strain, the modulus decreases rapidly. After undergoing large strains the modulus values converge to a single line.

The secant modulus is the slope of the stress-strain curve between the initial point and any other point (Lambe and Whitman, 1969). At the beginning of the shear portion of the test, the soil is still exhibiting elastic behaviour, as shown by the initial linear portion of the plots shown in below. The data below suggests that there is a general relationship between the maximum value of secant modulus and vertical effective stress; however, from the data presented below, it is evident that it does not normalize perfectly. A plot of the maximum secant modulus and vertical effective stress is shown in Figure 4:13.

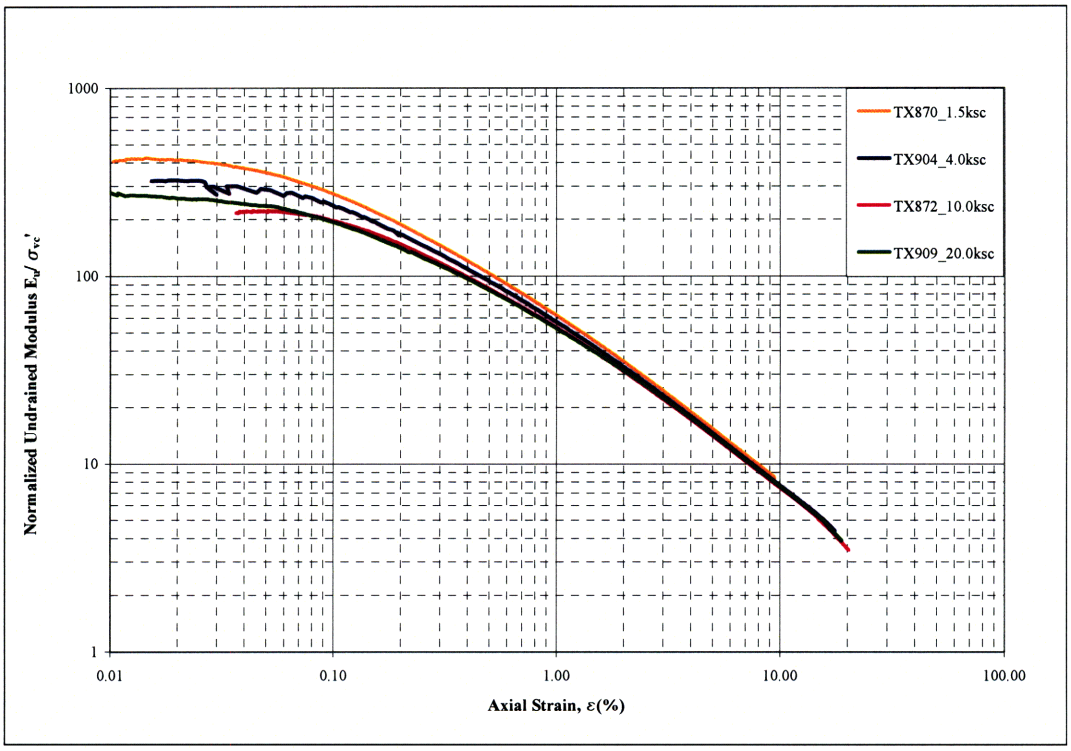

Figure 4:12 Normalized Secant Modulus (E_u) vs Axial Strain (ε%)

The following figure, Figure 4:13, shows the relationship between the maximum measure secant modulus (E_{max}) and the vertical consolidation effective stress (σ'_{vc}). This plots shows that there is a clear trend between E_{max} and σ'_{vc}. A relationship was proposed by Santagata (1999) relating these two variables and was presented as:

$E_{max} \propto \sigma_{vc}^{'\,0.74}$. To plot the dashed line shown in Figure 4:13, a proportionality constant of 450 was used, making the equation of the line: $E_{max} = 450 \times \sigma_{vc}^{'\,0.74}$. When compared to the measured values of E_{max} from the tests done as a part of this study, it can be seen that there is very good agreement.

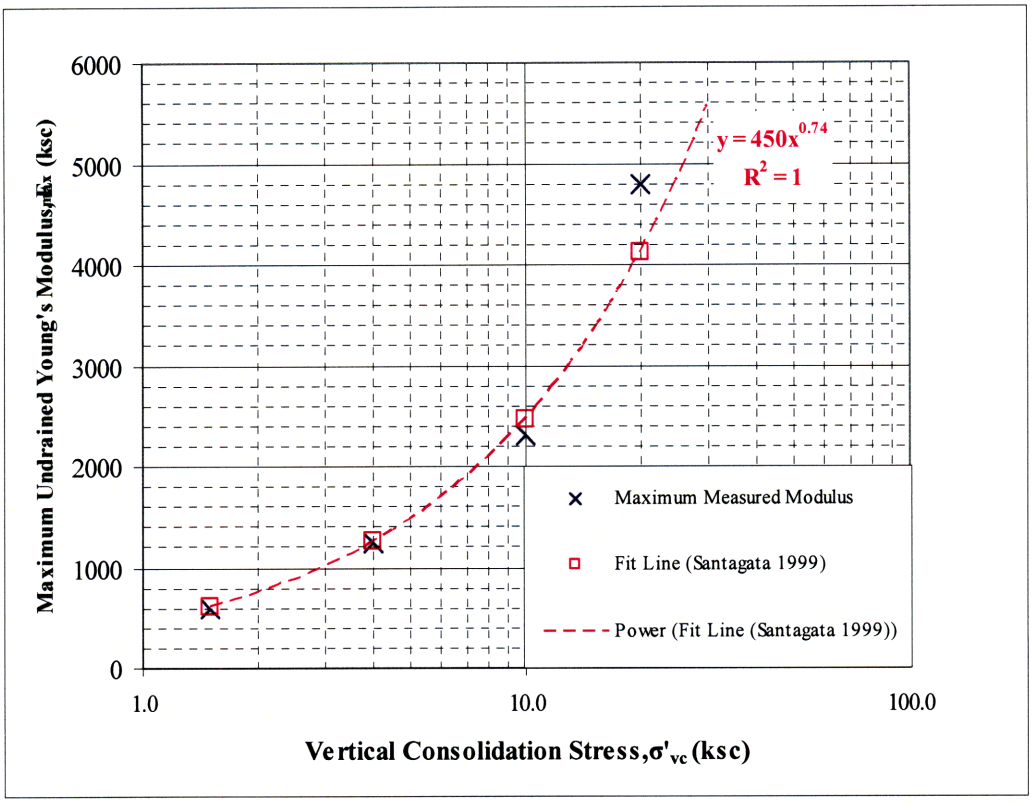

Figure 4:13 Maximum Secant Modulus (Emax) vs Vertical Consolidation Effective Stress (σ'_{vc})

The A Parameter and Axial Strain

The A parameter describes the slope of the undrained stress path with respect to the initial point (end of consolidation in the stress space) throughout the shearing portion of the test (Mazzei, 2008). For the specimens tested, the A parameter begins at 0.44 to 0.45, which is the expected starting value. After about 6% axial strain, the clay reaches more or less constant value of A = -0.15.

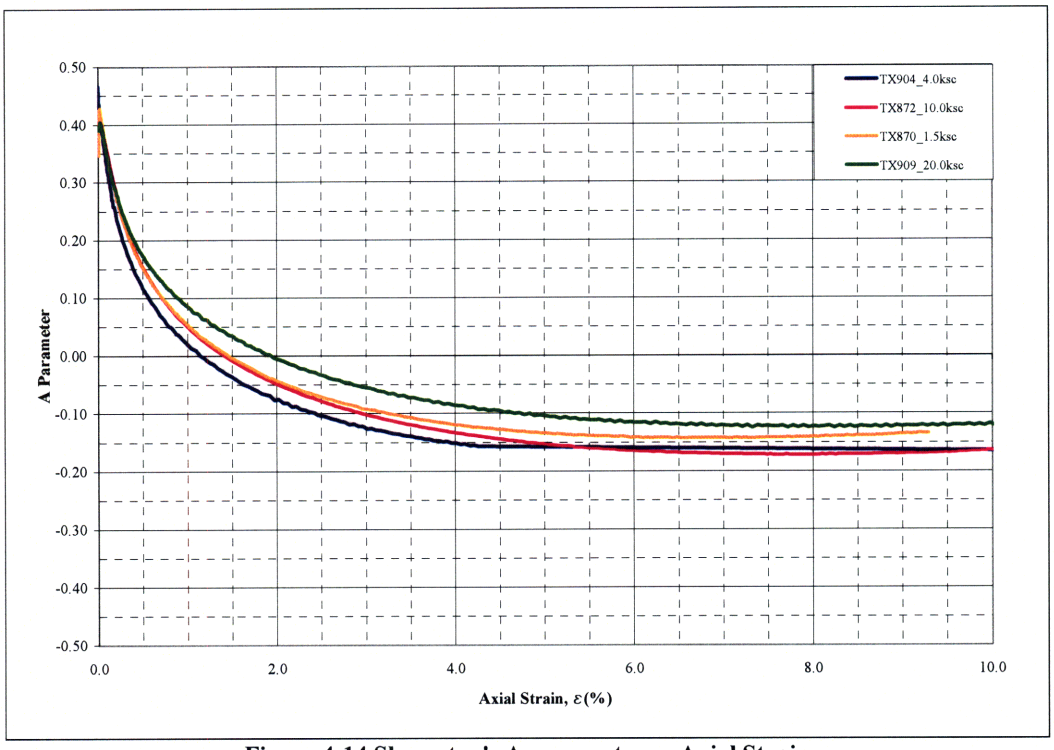

Figure 4:14 Skempton's A-parameter vs Axial Strain

Shear and Excess Pore Pressures and Axial Strain

Figure 4:15, shows the variation in excess and shear pore pressures with axial strain during the shear portion of the CK_0UE tests. During undrained shearing, excess and shear induced pore pressures build up within the specimen as drainage is not permitted. The excess pore pressure goes negative at first but then increases to a positive value before reaching a relatively steady value at large strains. In general, the excess pore pressures generated are small because, the ESP (Effective Stress Paths) is close to the TSP (Total Stress Paths) for these tests. The shear induced pore pressure is positive from the initial phases of axial strain. These relationships are also shown in Figure 4:15 below as the dashed lines. Although the values between the 1.5ksc and the 4.0ksc test are very close, the results generally show that there is a clear trend between the shear induced pore pressure and the vertical effective stress.

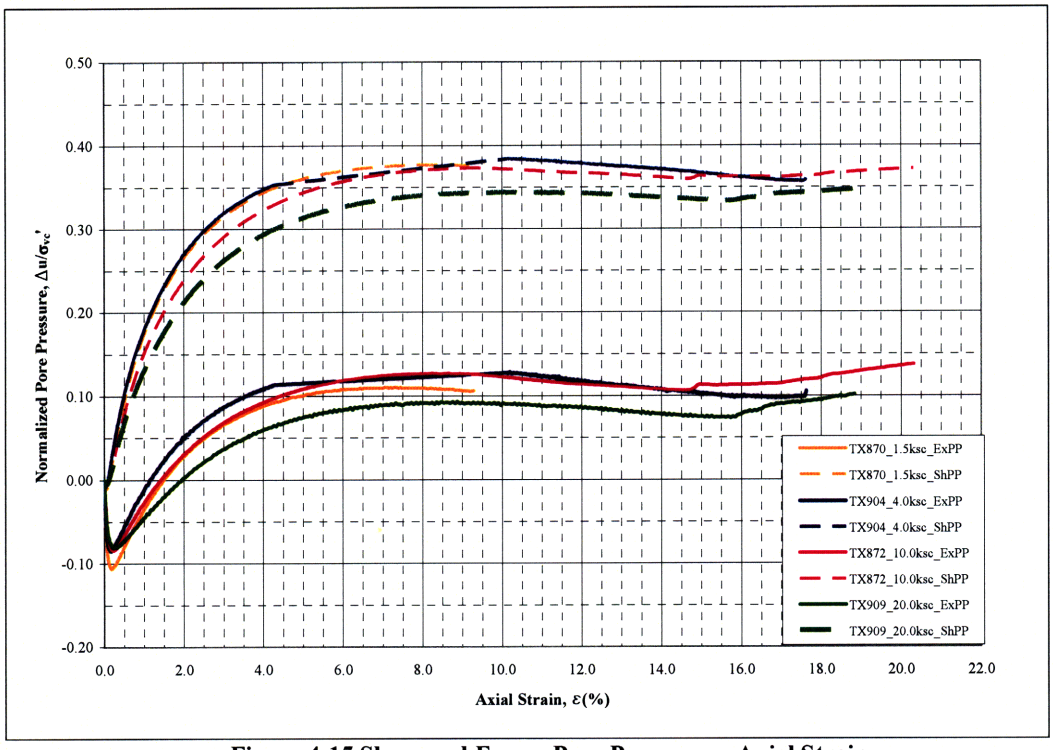

Figure 4:15 Shear and Excess Pore Pressure vs Axial Strain

Friction Angle and Axial Strain

The relationship between the friction angle (ϕ') and axial strain (ε%) during shearing is shown in Figure 4:16. This figure shows that the peak friction angle occurs after very large strains (~14%). After reaching peak a steady decrease in the friction angle is then observed. At these high levels of strain, the friction angle values become unreliable as large deformations and necking has begun to take place in the specimen.

As previously mentioned, and illustrated in Figure 4:6, the peak shear strength also occurs after 14% strain, which is unlike the behaviour observed during compression where the peak shear strength and peak friction angle do not occur at the same time or after the same amount of axial strain.

From this relationship the peak friction angles were determined (estimated for TX870) and plotted with vertical effective stress as shown in Figure 4:17. This figure shows that there is also a clear trend between the friction angle and the vertical effective stress level: the peak friction angle noticeably decreases (~25%) with the vertical effective stress < 10.0ksc, between 10.0ksc and 20.0ksc, the change in friction angle is not as large (~8% decrease).

Figure 4:17 also includes logarithmic equations best fitting the data. It is important to note that the data point for the peak friction angle at a stress level of 1.5ksc was an extrapolated data point taken from Figure 4:16.

Figure 4:18, shows the variation of the peak friction angle (ϕ'), with vertical consolidation effective stress (σ'_{vc}) for both compression and extension shear. The shear strength data from the extension tests was obtained from tests done as a part of this study; it is the shear strength data presented in Figure 4:17. The shear strength data from the compression tests was taken from Abdulhadi (2009), where CK_0UC tests were performed on Series IV RBBC. In general the shape of the trends are similar; the figure shows that the trends actually lie on top of one another for vertical effective stresses > 10.0ksc. For the vertical stresses <10.0ksc the difference in the values of peak friction angle are as much as 7^o for the same stress level.

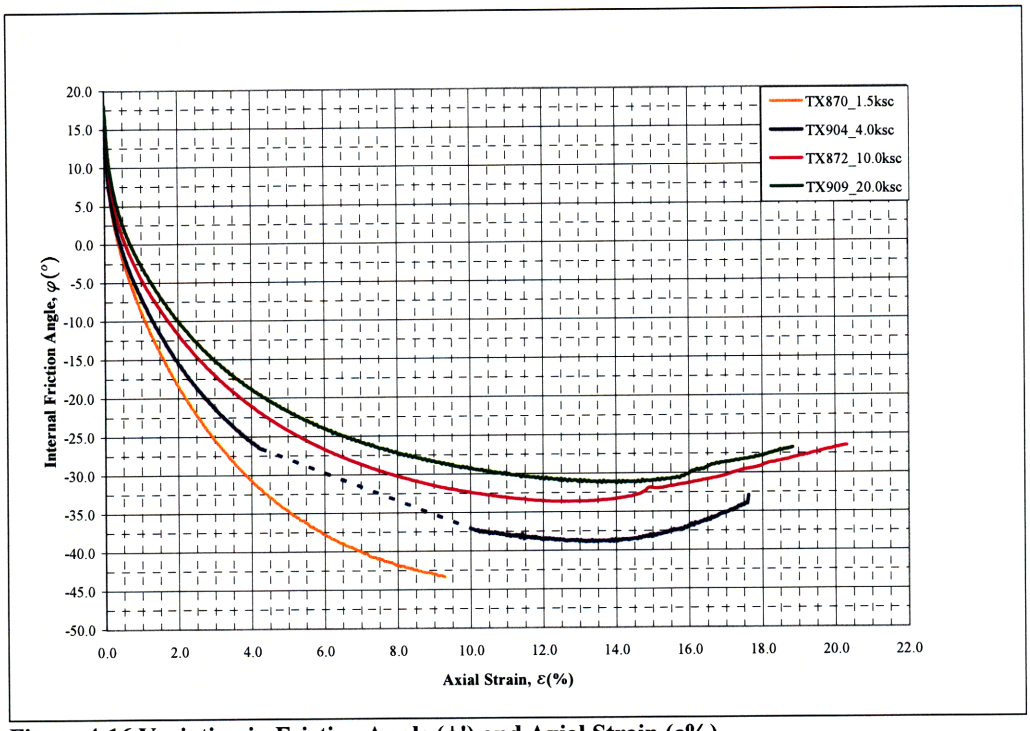

Figure 4:16 Variation in Friction Angle (ϕ') and Axial Strain (ε%)

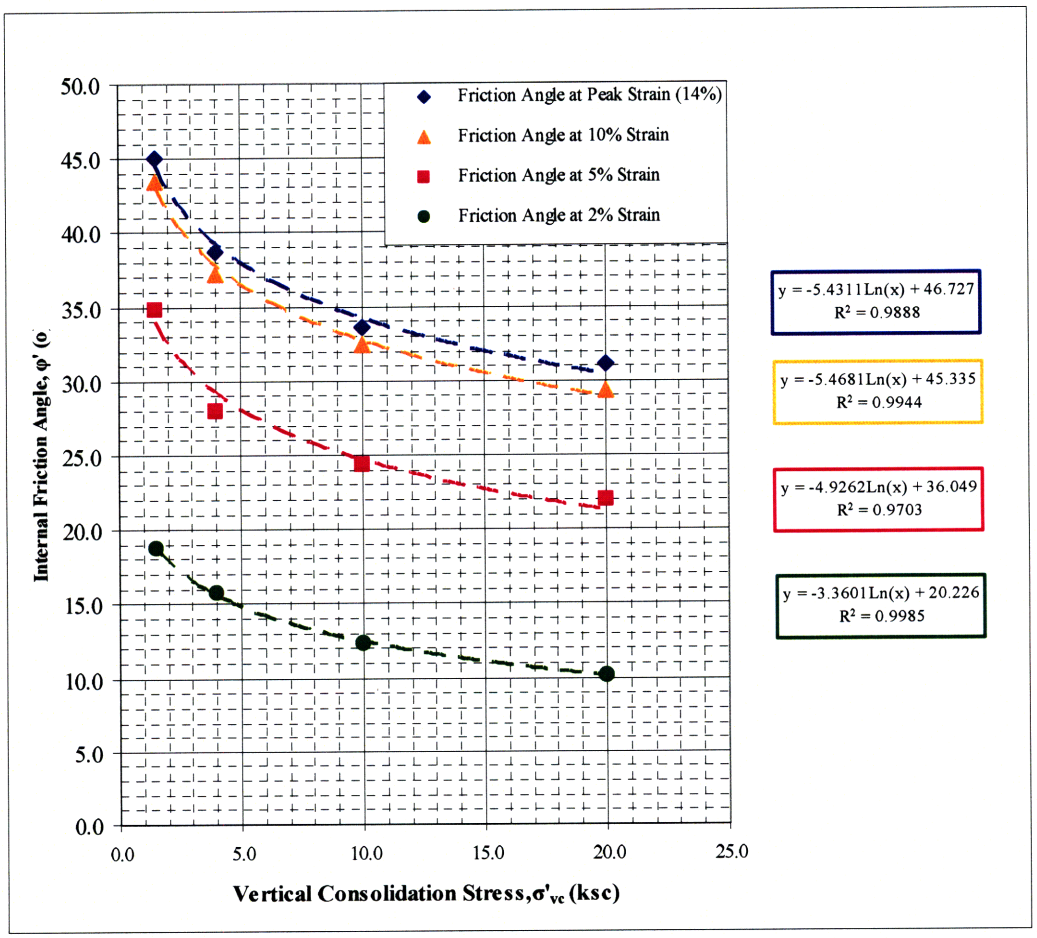

Figure 4:17 Friction Angle (ϕ') vs Vertical Effective Stress (ε%)

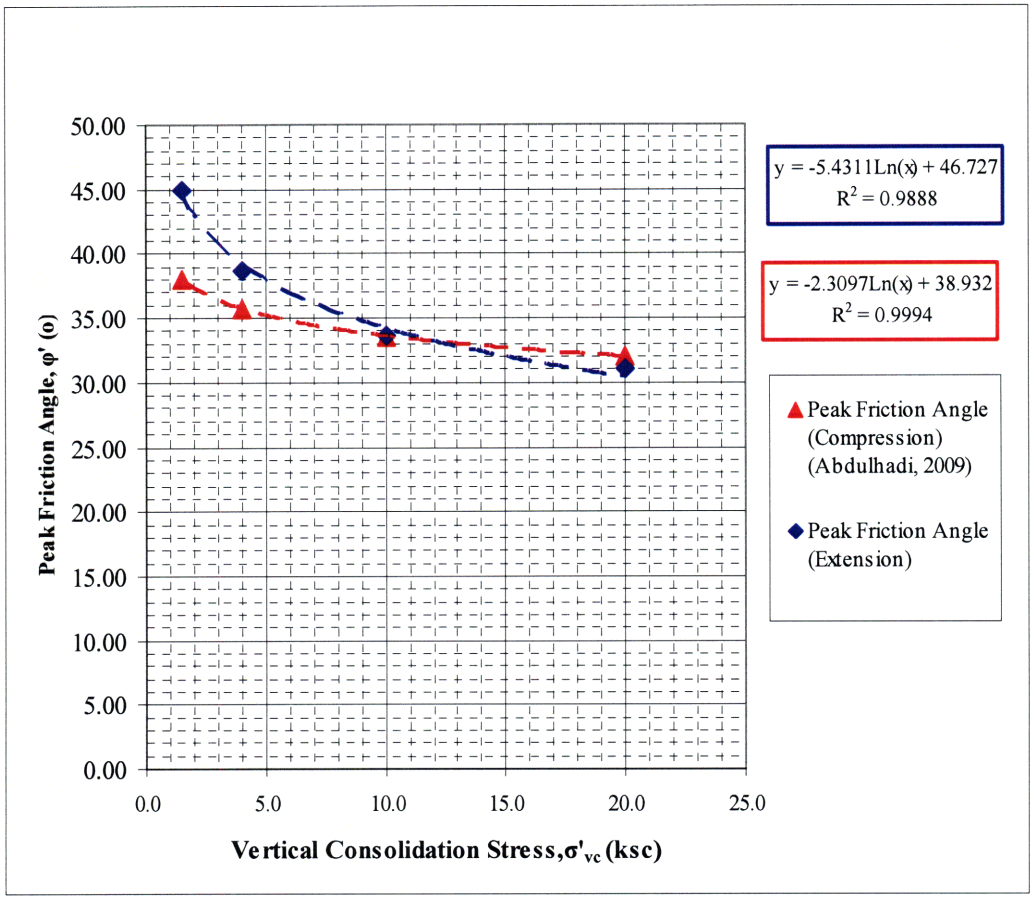

Figure 4:18 Peak Friction Angle (ϕ') vs Vertical Effective Stress (ε%) for Compression and Extension

Normalized Undrained Stress Path - MIT q-p' space

The following figure, Figure 4:20, shows the normalized stress paths during the shear portion for four of the tests done in this study. The axes are given by $q = \frac{1}{2}(\sigma_1 - \sigma_3)$ and $p' = \frac{1}{2}(\sigma'_1 + \sigma'_3)$. The starting point of each of the tests represents the stress state at the end of K_0 consolidation. In general, the geometry of the curves is very similar. For all of the curves, a mean stress of approximate 0.6ksc is attained as the stress paths cross the hydrostatic axis i.e. when the shear stress is zero. At the end of the stress paths, a variety of geometries is observed; the button-hook like curves are of different sizes. This may be due to the significant deformation observed in the specimen after failure.

Another point of note is that there is no obvious trend with stress level except at the at the end where lower stress lead to lower shear strains.

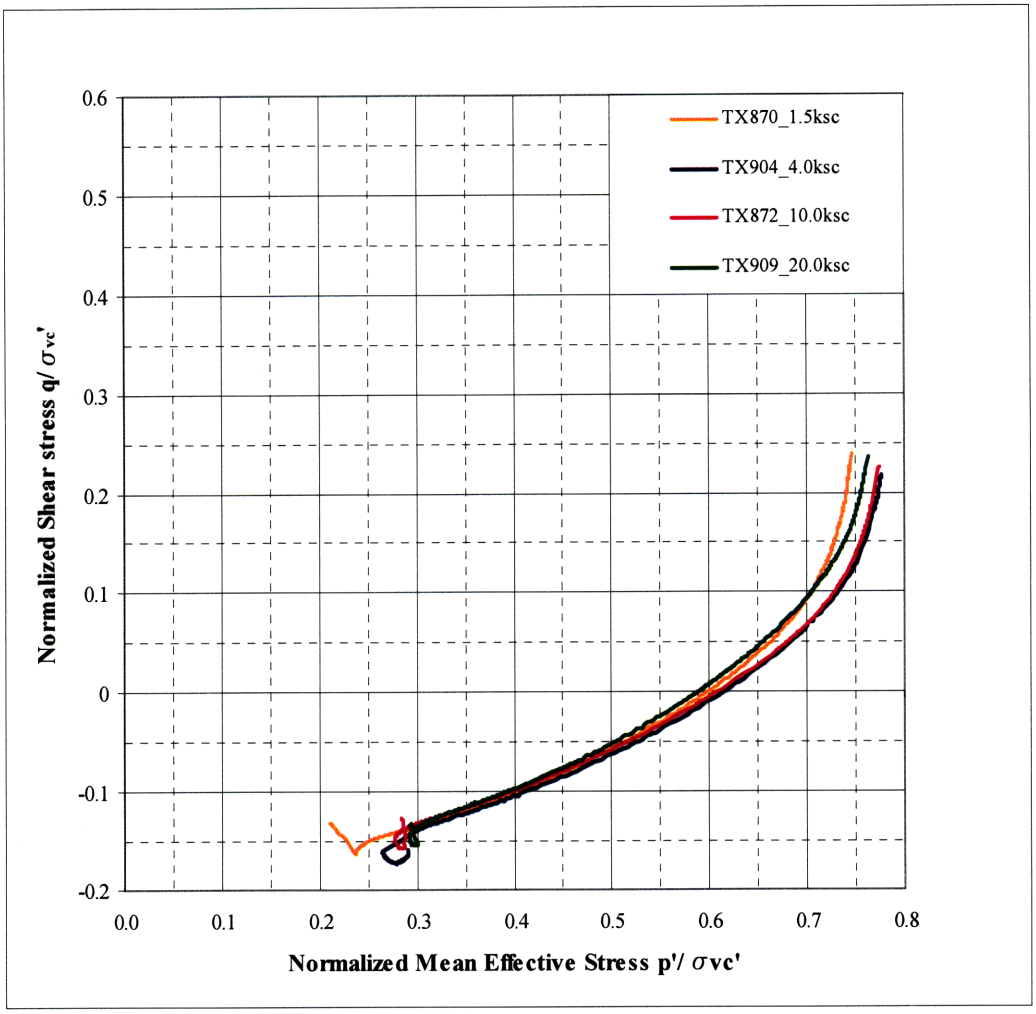

Figure 4:19 Normalized Undrained Shear Stress Paths

Undrained Stress Path - MIT q-p' space

The undrained shear stress paths are shown in Figure 4:20 below. The stress path plot shows the stresses that the specimen undergoes during load application. The axes are given by $q = \frac{1}{2}(\sigma_1 - \sigma_3)$ and $p' = \frac{1}{2}(\sigma'_1 + \sigma'_3)$. The shearing portion of the test begins after K_0 consolidation; the K_0 consolidation line is also shown. The specimens are then sheared to failure and the failure envelope can be deduced. From this plot, a friction angle (ϕ') of 25.8° and an apparent cohesion (c') of 0.085 ksc (8.3kPa) can be deduced as the undrained shear strength parameters.

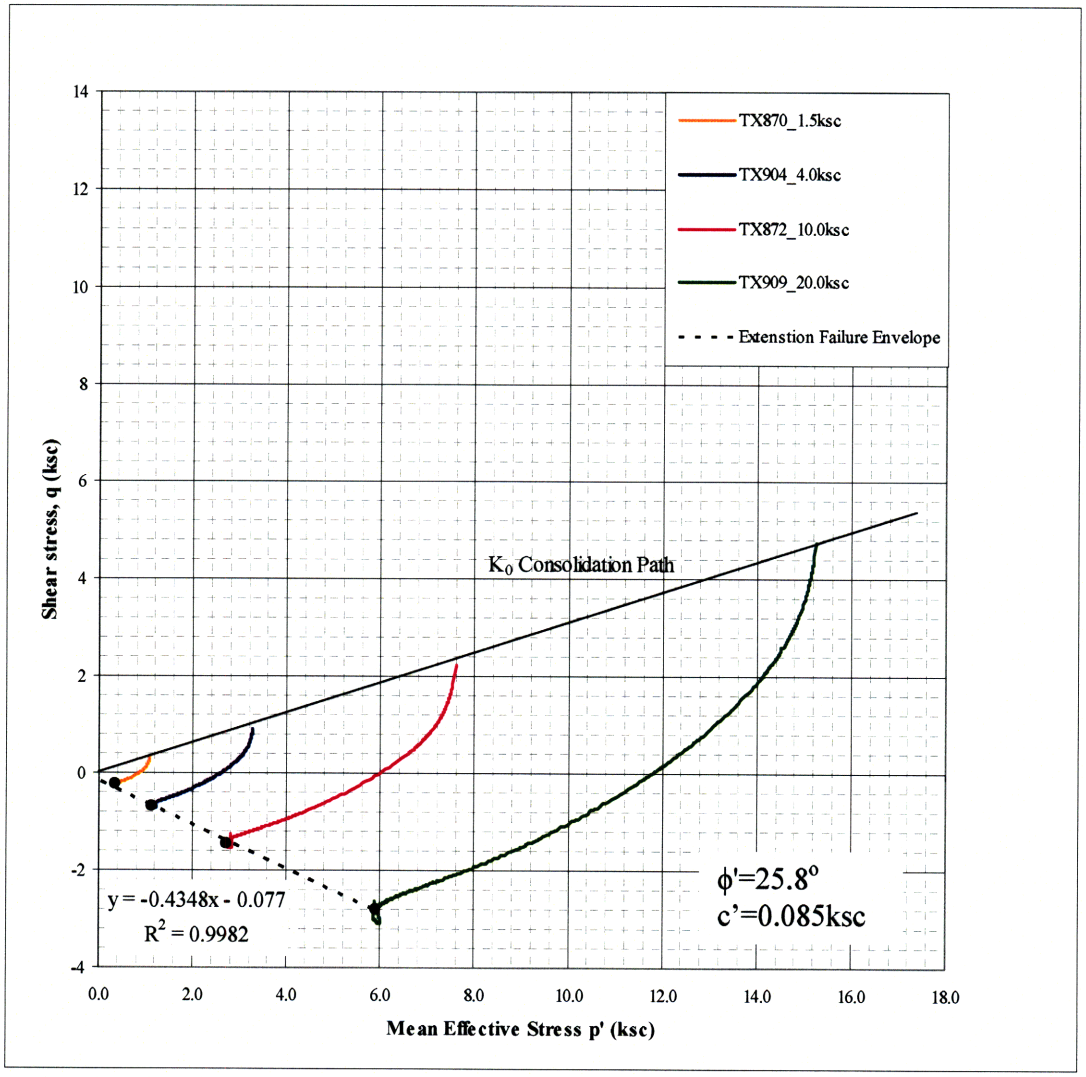

Figure 4:20 Undrained Shear Stress Path (q-p')

5.0 CONCLUSIONS & RECOMMENDATIONS

5.1 Conclusions

This portion of the chapter summarises the results obtained from eight hydrostatically consolidated undrained triaxial extension (CK_0UE) tests performed on Resedimanted Boston Blue Clay (RBBC).

Consolidation data were successfully collected from seven out of the eight tests at five different stress levels. The results show that the preconsolidation pressures measured from the consolidation data ranged from 0.85ksc to 1.15ksc.

The initial void ratios measured ranged from 1.16 to 1.24. It was found that they were fairly consistent with the initial void ratios, 0.86 to 1.22, obtained from the consolidation portion of the CK_0UC and CRS tests carried out by Abdulhadi (2009).

The compression index C_c ($=\Delta e/\Delta \log \sigma'_v$) values obtained from these tests ranged from 0.34 to 0.42. On average, these values are slightly higher than the C_c values (0.28 to 0.39) obtained from the consolidation portion of the CK_0UC and CRS tests carried out by Abdulhadi (2009), but are generally in good agreement.

The general trend observed with the lateral stress ratio was that as the specimen approached the preconsolidation pressure, the values of K_0 (the lateral stress ratio) reached a minimum and then increased slightly to a steady state value ranging from 0.54 to 0.56. This behaviour is typical of Series IV RBBC as shown in Figure 2:8 Lateral stress ratio versus vertical effective stress (σ'vc) during K0-consolidation of RBBC (Abdulhadi, 2009).

Shear data were successfully collected for four of the eight tests carried out. After the specimen has been K_0 consolidated to the desired vertical effective stress level, the specimen is then sheared in extension.

Upon plotting the stress strain data during shear in extension, it was found that, in general, the peak strength occurs after an axial strain of approximately 14%. This strain level is large compared to the strain level at which the peak strength is typically observed in compression (~1%).

The aim of this study was to explore the relationship between vertical consolidation stress and the undrained shear strength behaviour in extension for cohesive soils to determine whether the normalized soil parameter concept (and hence SHANSEP) is still applicable at vertical consolidation stresses ranges of $\sigma'_v \geq 1.0$MPa. The results clearly show that stress level does have an impact on the undrained shear strength in extension.

To clearly show the variation in the normalized shear stress level (q/σ'_{vc}) with vertical effective stress level, the shear stress levels at various strains (attained from Figure 4:7), were plotted and illustrated in Figure 4:9. The normalized peak shear strength (also called the undrained shear strength ratio, S_u/σ'_{vc}) was also plotted on this chart. There is a very clear trend that can be observed from Figure 4:9; the undrained shear stress level, and consequently, the undrained shear strength, decreases with vertical effective stress. Results from these tests clearly show that the undrained shear strength decreases with vertical effective stress. The undrained shear strength decreased from 0.17 ksc to 0.15 ksc, corresponding to an increase in vertical consolidation stress level from 4.0 ksc (0.4 MPa) to 20.0ksc (2.0 MPa).

The variation of the undrained shear strength ratio, (S_u/σ'_{vc}), with vertical consolidation effective stress (σ'_{vc}) for both compression and extension shear was plotted and presented in Figure 4:11. The shear strength data from the compression tests was taken from Abdulhadi (2009), where CK_0UC tests were performed on Series IV RBBC. This figure shows clearly the anisotropy associated with shear strength in compression and extension. Using these results, the shear strength in compression is 1.74 to 1.90 times greater than the shear strength obtained from the extension tests.

The variation of the peak friction angle (ϕ'), with vertical consolidation effective stress (σ'_{vc}) for both compression and extension shear was also plotted and is presented in Figure 4:18. The shear strength data from the extension tests was obtained from tests done as a part of this study; it is the shear strength data presented in Figure 4:17. The shear strength data from the compression tests was taken from Abdulhadi (2009), where CK_0UC tests were performed on Series IV RBBC. In general the shape of the trends are similar; the figure shows that the trends actually lie on top of one another for vertical effective stresses > 10.0ksc. For the vertical stresses <10.0ksc the difference in the values of peak friction angle are as much as 7^o for the same stress level.

It should also be mentioned here that there was no discernable trend between the lateral stress ratio (K_0) and the undrained shear strength (S_u).

5.2 Recommendations for Future Research

From the results of this study it is apparent that the undrained shear strength in extension decreases with vertical consolidation effective stress. However, these conclusions were based on the results of a fairly small data set. Before these trends can be generally accepted and applied to practice, it is recommended that further tests be carried out, a bigger data set to be obtained, to concretize the results.

The future tests should be carried out in the lower stress range, <10.0ksc, given that is where the greatest change in strength with stress level occurs. In addition, more tests should be carried out at stress levels >20.0ksc to observe whether the trend eventually reaches a steady state value or if it continues to decrease.

It is also recommended that tests be carried out with lubricated ends to observe whether this has any impact on the development of the failure plane or any impact on the strength data.

REFERENCES

Abdulhadi, N.O. (2009, expected) Untitled Ph.D Thesis, MIT, Cambridge

Ahmed, I. (1990). "Investigation of Normalized behaviour of Resedimented Boston Blue Clay Using Geonor Direct Simple Shear Apparatus", S.M. thesis, MIT, Cambridge, MA,372pp

Bjerrum, L. (1969). "Effect of Rate of Strain on Undrained Shear Strength of Soft Clays", Proceedings, 7th ICSMFE, Mexico City, Panel Discussion 5.

Germaine, J.T. (2007). "1.37 Geotechnical Measurements and Exploration Class Notes." MIT, Cambridge, MA

Germaine, J.T. (1982), "Development of the Directional Shear Cell for Measureing Cross Anisotropic Clay Properties," Doctor of Science Thesis, Department of Civil Engineering, MIT, Cambridge, MA.

Jamiolkowski, M., Ladd, C.C., Germaine, J.T., and Lancellotta, R. (1985), "New developments in Field and Laboratory testing of Soils," Proc. XI ICSMFE, San Francisco, Vol. I, pp. 57-153

Ladd, C.C. (2007). "1.361 Soil Mechanics (MIT): Class Notes." MIT, Cambridge, MA

Ladd, C.C., (1964). " Stress-Strain Behavior of Saturated Clay and Basic Strength Principles." Dept. of Civil Engineering, MIT, Cambridge, MA, 105 pp.

Ladd, C.C., Foot, R. (1974). " New Design Proceedure for Stability of Soft Clays." Dept. of ASCE, JGED, Vol.100, No. GT7,763 – 786pp.

Ladd, C.C., Lambe, T.W. (1968). "The Strength of Undisturbed Clay Determined from Undrained Tests" Special Technical Publication No. 361, National Research Council of Canada-American Society of and Materials Symposium on Laboratory Shear Testing of Soils, 1968, 342-371pp.

Lambe, T.W., Whitman, R.V., (1969). "Soil Mechanics," John Wiley & Sons, New York City, NY, USA, 553 pp.

Mazzei, D.P.C., (2008). "Normalized Mechanical Properties of Resedimented Gulf of Mexico Clay from Integrated Ocean Drilling Program Expedition Leg 308" M.Eng. Thesis, Dept. of Civil Engineering, MIT, Cambridge, MA, 137 PP.

Roscoe, K.H., A.N. Schofield and C.P. Wroth (1958). "On Yielding of Soils", Geotechnique, Vol. 8, pp. 22-53

Roscoe, K.H. and J.B. Burland (1968). "On the Generalized Stress-Strain Behaviour of 'Wet' Clay" in Engineering Plasticity, J. heyman and F.A. Leckie, eds., pp. 535-609

Santagata, M.C., (1999). "Factors Affecting the Initial Stiffness and Stiffness Degradation of Cohesive Soils," Ph.D. thesis, Dept. of Civil and Environmental Engineering, MIT, Cambridge, MA, 337 pp.

Sheahan, T.C., (1991). "An Experimental Study of the Time-Dependent Undrained Shear Behavior of Resedimented Clay Using Automated Stress Path Triaxial Equipment," Sc.D. thesis, Dept. of Civil Engineering, MIT, Cambridge, MA, 952 PP.

Whittle, A.J., Kavvadas, M., (1994) "MIT-E3: A constitutive model for overconsolidated clays", *J Geotech Eng, ASCE* **120** (1), pp. 173–198

APPENDIX I

Summary of Triaxial Consolidation Results

Last Revised: 05/26/2009

Spec. Location		Index Tests			Specimen Data		Conditions			Consolidation Results						Remarks
										General		@ Max Stress		@ Preshear		
Test #	Depth	T_v	ω_n	ω_p	ω_n	e_i	σ'_i	u_b	B	σ'_p	CR	ε_a	σ'_{vm}	ε_a	σ'_{vc}	
Boring		SD	SD	ω_l	I_p	S_i						ε_{vol}	K_c	ε_{vol}	OCR	
				%2						ε_a/h						
Sample	Markers	# obs	# obs	μ	γ_t	G_s	ε_a	ε_a	ε_{vol}	r	RR	C_α	t_s	K_c	t_s	
TX870	RBBC		41.03		40.46	1.206	0.30	2.98	93	1		4.74	1.439	4.74	1.439	K_0 consolidation
	SA1		1.09			92.2						4.43	0.504	4.43	1.000	
MIT02			3		1.771	2.70	0.09	0.07	-0.84	0.15			27.0	0.504	27.0	
TX872	RBBC		43.13		45.01	1.222	0.17	3.05	93	1		18.59	9.856	18.59	9.86	K_0 consolidation
	SA2		0.72			102.40						18.70	0.548	18.70	1.000	
MIT02			2		1.814	2.70	-0.05	0.01	-0.65	0.15			17.2	0.548	17.2	
TX875	RBBC		43.34		43.16	1.166	0.27	2.89	90	1		20.73	19.838	20.73	19.838	K_0 consolidation
	SA3		1.29			102.9						20.73	0.557	20.73	1.000	
MIT02			3		1.837	2.70	-0.08	0.00	-0.96	0.15			5.3	0.557	5.3	
TX883	RBBC		42.63		43.69	1.198	0.24	2.93	92	1		22.09	19.958	22.09	19.958	K_0 consolidation
	SA4		0.7			101.37						22.27	0.572	22.27	1.000	
MIT02			2		1.817	2.70	-2.62	-1.56	-1.82	0.15			26.3	0.572	26.3	

Table A:1 Summary of Triaxial Consolidation Results

Summary of Triaxial Consolidation Results

Spec. Location		Index Tests			Specimen Data		Conditions			Consolidation Results						Remarks
										General		@ Max Stress		@ Preshear		
Test #	Depth	T_v	ω_n	ω_p	ω_n	e_i	σ'_i	u_b	B	σ'_p	CR	ε_a	σ'_{vm}	ε_a	σ'_{vc}	
Boring		SD	SD	ω_l	I_p	S_i						ε_{vol}	K_c	ε_{vol}	OCR	
		#		%2						ε_a/h	RR					
Sample	Markers	obs	# obs	μ	γ_t	G_s	ε_a	ε_a	ε_{vol}	r		C_α	t_s	K_c	t_s	
TX899	RBBC SA5		42.45 0.19		43.38	1.203 100.26	0.28	3.02	99	1					1.000	K_0 consolidation
MIT02			3		1.809	2.70	-0.23	-0.11	-22.98	0.15						Consolidation Data Unreliable
TX903	RBBC SA6		42.88 0.31		43.59	1.224 98.99	0.30	3.05	97	1		6.72 6.84	1.87 0.485	6.72 6.84	1.870 1.000	K_0 consolidation
MIT02			3		1.795	2.70	-0.14	-0.20	-2.02	0.15			24.6	0.485	24.6	
TX904	RBBC SA7		42.94 0.4		45.51	1.209 104.67	0.31	2.96	100	1		9.74 9.69	4.219 0.558	9.74 9.69	4.219 1.000	K_0 consolidation
MIT02			4		1.831	2.70	-0.61	-0.58	2.55	0.15			6.13	0.551	6.13	
TX909	RBBC SA8		42.61 0.76		43.9	1.241 98.37	0.27	2.94	100	1		22.32 22.16	20.009 0.527	22.32 22.16	20.009 1.000	K_0 consolidation
MIT02			4		1.785	2.70	-0.02	-0.06	-0.11	0.15			36.8	0.527	36.8	

Table A:1 Summary of Triaxial Consolidation Results

Summary of Triaxial Undrained Shear Results

Last Revised: 05/26/2009

Specimen Location		Specimen Data		Conditions			At Max Shear			At Max Obliquity			E_u @		Remarks
													ε_a =	$\Delta q/\Delta q_m$	
Test #	Depth	ω_n	e_i		e_c	σ'_{vc}	ε_a	$\Delta u_e/\sigma'_{vc}$	q/p'	ε_a	$\Delta u_e/\sigma'_{vc}$	q/p'	0.01%	0.3	
Boring	□	I_p	S_i	ε_a/hr				$\Delta u_s/\sigma'_{vc}$	ϕ'		$\Delta u_s/\sigma'_{vc}$	ϕ'	0.1%		
Sample	Markers	γ_t	G_s	□	K_c	OCR	q_f/σ'_{vc}	p'_f/σ'_{vc}	A	q_f/σ'_{vc}	p'_f/σ'_{vc}	A	1.0%	0.5	
TX870		40.46	1.206			1.439	-9.39	0.1049	-0.688	-9.39	0.1049	-0.688	403.507	299.267	
0			92.2	-0.5				0.3758	-43.5		0.3758	-43.5	273.525		
MIT02	0.00	1.771	2.70		0.504	1.00	-0.1632	0.2372	-0.1341	-0.1632	0.2372	-0.134	61.864	167.979	
TX872		45.01	1.222			9.856	-13.72	0.1082	-0.551	-13.72	0.1082	-0.551	N/A	182.390	
0			102.4	-0.5				0.36287	-33.4		0.3629	-33.4	196.581		
MIT02	0.00	1.814	2.70		0.548	1.00	-0.1565	0.2839	-0.142	-0.1565	0.2839	-0.142	52.749	102.384	
TX875		43.16	1.166			19.838									
0			102.9	-0.5											
MIT02	0.00	1.837	2.70		0.557	1.00									
TX883		43.69	1.198			19.958									
0			101.4	-0.5											
MIT02	0.00	1.817	2.70		0.572	1.00									

a) Marker location in tube

b) Stresses in kg/cm^2

c) 1 kg/cm^2 = 2048 psf

d) Depth in Feet

e) Time in hours

f) Water content, saturation, and strain in %

g) density in gm/cm^3

Table A:2 Summary of Triaxial Shear Results

Summary of Triaxial Undrained Shear Results

Last Revised: 05/26/2009

Specimen Location		Specimen Data		Conditions			At Max Shear			At Max Obliquity			E_u @		Remarks
													ε_a =	$\Delta q/\Delta q_m$	
Test #	Depth	ω_n	e_i		e_c	σ'_{vc}	ε_a	$\Delta u_e/\sigma'_{vc}$	q/p'	ε_a	$\Delta u_e/\sigma'_{vc}$	q/p'	0.01%	0.3	
Boring	□	I_p	S_i	ε_a/hr				$\Delta u_s/\sigma'_{vc}$	ϕ'		$\Delta u_s/\sigma'_{vc}$	ϕ'	0.1%		
Sample	Markers	γ_t	G_s	□	K_c	OCR	q_f/σ'_{vc}	p'_f/σ'_{vc}	A	q_f/σ'_{vc}	p'_f/σ'_{vc}	A	1.0%	0.5	
TX899		43.38	1.203			0.000									
0			100.3	-0.5											
MIT02	0.00	1.809	2.70		0.000	1.00									
TX903		43.59	1.224			1.870									
0			98.99	-0.5											
MIT02	0.00	1.795	2.70		0.485	1.00									
TX904		45.51	1.209			4.219	-14.98	0.10137	-0.620	-14.98	0.1014	0.620	510.504	261.250	
0			104.7	-0.5				0.36621	-38.0		0.3662	-38.0	242.319		
MIT02	0.00	1.831	2.70		0.551	1.00	-0.1725	0.2783	-0.128	-0.1725	0.2783	-0.128	55.112	139.593	
TX909		43.9	1.241			20.009	-14.66	0.0747	-0.518	-14.66	0.0747	0.518	276.952	166.555	
0			98.37	-0.5				0.3352	-31.2		0.3352	-31.2	192.079		
MIT02	0.00	1.78534	2.70		0.527	1.00	-0.154	0.2975	-0.096	-0.1540	0.2975	-0.096	52.079	94.866	

a) Marker location in tube

b) Stresses in kg/cm^2

c) 1 kg/cm^2 = 2048 psf

d) Depth in Feet

e) Time in hours

f) Water content, saturation, and strain in %

g) density in gm/cm^3

Table A:2 Summary of Triaxial Shear Results